COO-1549-15

Technical Progress Report

NUCLEAR PHYSICS STUDIES USING NUCLEAR EMULSIONS

Contract Number AT(11-1)-1549

November 6, 1965 through October 31, 1969

between

The United States Atomic Energy Commission

and the

University of Wyoming, Laramie, Wyoming

DISCLAIMER

I. INTRODUCTION

This report summarizes the work performed during the period November 6, 1968 through October 31, 1969 under Contract AT(11-1)-1549 between the University of Wyoming and the U.S. Atomic Energy Commission. In addition to the projects discussed in the previous progress report, the expansion of our efforts into high precision gamma ray spectroscopy and activation analysis are discussed.

II. GAMMA RAY SPECTRUM FROM Ga^{64}

S. Browne and H. B. Eldridge, University of Wyoming
and
C. S. Zaidins, University of Colorado

As discussed in the previous progress report, a search for the isotope Ge^{64} was initiated. The first attempt: $Zn^{64}(He^3,3n)Ge^{64}$ with the measurements of the half life of the granddaughter Zn^{64} gamma rays was not successful. This procedure was necessary since the Ga^{64} lines were not known. As our next step, it was decided to measure the energies of the Ga^{64} lines; however, this required a n,γ coincidence experiment. As our second experiment, 16 Mev protons produced at the cyclotron of the University of Colorado at Boulder, Colorado, were directed along a zero-degree beam to impinge upon a thin target of Zn^{64}. The reaction

$$Zn^{64}(p,n)Ga^{64*}$$

occurred to produce an excited state of Ga^{64} which immediately (10^{-22}sec.) decayed to the ground state, accompanied by the emission of a gamma ray.

Detection of this de-excitation gamma was attempted using a lithium-drifted germanium diode reverse biased at 600 Volts; its high energy resolution ($\sim$ 3 Kev) made it ideal for an accurate measurement. But to insure that only Ga^{64} gammas were measured, a coincidence was established with the gallium-creating neutron expulsion. A stilbene scintillator optically coupled to an RCA photo-multiplier tube was used to detect neutrons; the 10th dynode was fed to an Elron PSD-N-1 Pulse-Shape Discriminator which distinguished between the "fast" gamma pulses and the "slow" neutron pulses produced in the stilbene. With a 1000:1 rejection ratio for gammas in the "slow" output, with a full spectrum (down to 100 Kev) of neutron recognition, we were assured of detecting only coincidence neutrons.

Coincidence itself was established with the fast outputs of both the stilbene and Ge(Li) detectors. A Time Pickoff unit connected to the anode of the photomultiplier marked the rise of a stilbene pulse; this signal (when properly delayed) initiated the sweep of a Time-to-Pulse-Height Converter. The sweep was halted by the zero-crossing output of a single-channel analyzer connected to the Ge(Li) detector's Linear Amplifier.

The timing for coincidence was adjusted by using a 10 μc Na^{22} source between the two obverse detectors. The annihilation reaction produced true γ-γ coincidence which could then be timed. The output of the Time-to-Pulse-Height Converter was displayed on a multi-channel analyzer. The three peaks represent different logic delays in the stilbene circuit, 250 nanoseconds apart. The central peak, with a full width at half maximum of less than 30 nanoseconds, was used. This spread is due to the non-consistent delays in the various systems, such as walk in the zero-crossing analyzer.

A single-channel window was placed on the output of the Time-to-Pulse-Height Converter. The window was adjusted to allow 50 nanoseconds to be counted on either side of the central (coincidence) peak. The logic pulses from this window indicated stilbene-Ge(Li) coincidence; it was and-gated with the appropriatel delayed pulse from the Pulse Shape Discriminator which indicated neutron detection in the stilbene. Thus, our final logic signal guaranteed neutron detection and coincidence; this was used in a coincidence mode to gate the 1024-channel Pulse Height Analyzer whose linear signal was the properly delayed pulse from the Ge(Li) amplifier.

There were several geometric difficulties encountered with this system. The desirability of maximum detector solid angle presented to the zinc target suggested moving the detectors close in; but high-intensity radiation from the bombarded target area distorted the Ge(Li) pulses enough to impair the detector's energy resolution. A compromise of 6" from the target for the Ge(Li) and 2" from the target for the stilbene was reached. In addition, the stilbene was placed almost in line with the beam, assuming that conservation of momentum dictated the emitted neutrons would appear in the same direction as the incident protons. An extremely low-intensity proton beam irradiated the target, thus minimizing unwanted excess radioactivity from the target area.

Having incorporated all these compromises, the tight coincidence network reduced the operating experiment to 3 counts per minute. A six-hour run yielded

about 1000 counts, and when this was spread over 1024 channels, the statistical deviation per channel turned out quite high. Thus, to date, no definite peaks have been observed in the spectrum. However, longer runs (36 hours) in the future should reveal the desired spectrum with sufficient accuracy to distinguish the characteristic Ga^{64} de-excitation gamma rays.

This work was presented as a paper at the meeting of the American Nuclear Society, Albuquerque, New Mexico, April 26, 1969

III. NEUTRON SPECTROMETER CONSTRUCTION

H. B. Eldridge — University of Wyoming
C. S. Zaidins — University of Colorado

A. Efficiency Studies

This project has been left in the same state as the last progress report awaiting the development of the burst selection system at the Colorado Cyclotron.

B. γ-Background Reduction

This project is essentially completed and resulted in a publication: Health Physics, Vol. 16, pp. 765-769. This publication is included in the appendix.

IV. A Determination of the Absolute Efficiency of Various Size Ge(Li) Gamma Ray Detectors In the Energy Range 60 to 2734 Kev.

J. Jarmer and H. B. Eldridge, University of Wyoming.

Several research projects in the accelerator laboratory at the University of Wyoming involve measuring the absolute intensity of gamma lines in a complex spectrum. In order to measure the absolute intensity accurately, detector efficiency as a function of gamma ray energy must be known.

In principle, one could calculate the absolute efficiency since the cross sections for ionization, Compton scatter, and pair production are known. The problem with making an accurate calculation is that one must know accurately the size and shape of the sensitive volume. Since this information is usually not available, it is easier to measure the efficiency experimentally for a given geometry.

In the energy range under consideration (60-2734 Kev) the gamma ray can interact with the germanium detector by photoelectric absorption, Compton scattering, or pair production. The photoelectric effect would be most prominent at

lower energies and except for the irregular behavior near the K, L, M x-ray absorption edges, would decrease with energy. The Compton effect shows a similar behavior; however, the pair production increases with energy above the threshold at 1.02 Mev. The net result of all the above types of interaction is that the total probability of interaction which is proportional to the efficiency should decrease with increasing gamma ray energy for a given size detector and solid angle. The detector size would of course affect the efficiency such that the efficiency should decrease as the size decreases.

The method involves measuring the activity (gamma ray emission rate) of several calibrated sources for which the activity is accurately known. The absolute efficiency is then defined as the ratio of the measured activity to the activity of the calibrated source for a given geometry.

Three Ge(Li) detectors of different volumes were used in the investigation. Two of the detectors had volumes of 22.4 and 4.6 cc. respectively. The third detector had an unknown volume but was thought to be 20 cc. Each detector was mounted in its own cryostat and connected through a pre-amplifier to an amplifier and then to a 4096 channel pulse height analyzer. Figure IV-1 shows one of the detectors. The large dewar contains the liquid nitrogen and the detector is located on top of the dewar. Figure IV-2 shows the multi-channel analyzer and screen of the oscilloscope. The rest of the equipment shown in this figure is used for other experiments.

Eight calibrated sources were borrowed from the University of Colorado. Each source was mounted 10 cm. from the detector and its gamma spectra was accumulated and stored on magnetic tape at the University of Wyoming Computer Center. Computer programs were written to help in the data analysis. With the aid of the programs the peaks in the spectrum of each foil were located, background subtracted off, area under the peaks determined and activity calculated by dividing the area under the peak by the count time. The measured activity for each line was then corrected for activity at the time the source was calibrated to obtain the absolute efficiency.

Figure IV-3 is a typical page from the computer output. The ordinate gives the number of counts and the abcissa is the channel number which can be read directly as energy in Kev. The plot shows how the computer fits the background to the peak.

The results are shown in Figure IV-4. Figure IV-4 is a semi-log plot of the

absolute efficiency as a function of energy. The curves were drawn by eye to fit the experimental points. The points were not corrected for 4π geometry nor were the low energy points corrected for absorption. The error bars are smaller than the size of the points. The errors were due to three causes: 1) statistical error in the number of counts; 2) error in the activity of the calibrated sources; and 3) error in the area under the peaks due to background fit.

An interesting result was obtained by comparing the measured efficiencies of our detectors with the efficiencies published by Walford and Doust for detectors of the same size. We found that the efficiency of our 22.6 cc. detector corresponded to a detector of 23 cc. according to Walford and Doust, and our 4.6 cc. detector corresponded to about a 3 cc. Since the volume of our third detector was not accurately known, its efficiency was compared to the published results and its volume was found to be about 8 cc.

When the analysis of the full energy to double escape peaks are completed, a publication of this work is planned for Nuclear Instruments and Methods.

This work was presented as a paper at the A.A.A.S. meeting in Colorado Springs, Colorado May 7, 1969.

V. Activation Analysis of Vanadium in Residual Oil

J. P. Flaherty and H. B. Eldridge, University of Wyoming

The Accelerator Laboratory's aid has been solicited to investigate the possibility of using activation analysis as a means of quantitatively determining trace element concentrations in crude oil at various stages of the refining process. The interest arose from another research group which was in the process of developing suitable commercial techniques to reduce the sulfur content in crude oil which had the more volatile constituents such as gasoline retorted out of it. The oil left after the retorting, most commonly called residual oil, is used for fuel oil purposes once the sulfur content is lowered to a safe value. The basic technique they employed was the passing of this oil through a cobalt-molybdate catalyist which withdrew the sulfur along with several trace metals. In their analysis they determined that the trace element, vanadium, was the primary element other than sulfur which was being extracted from the crude oil and that it, vanadium, was coating the catalyist and subsequently poisoning it at a faster rate then was desired. Hence, they were interested in determining the rate of extraction of the vanadium from the oil. The vanadium also was of interest because there was the possible interesting side feature,

that if enough vanadium and other trace elements were being deposited on the catalyist, it might be economically profitable to extract these metals from the catalyist after it had become impotent due to this poisoning.

We proposed to the chemists the possibility of using the methods of neutron activation analysis in their measurements of vanadium concentrations. This technique seemed to have two major attributes which would avail themselves nicely to their needs. One was the sensitivity of the method which would allow them to measure small concentrations very accuratedly. The second being the rapidity of the method which would lend itself to commercial on-line applications. We subsequently obtained several samples from them and embarked on the analysis.

The theory involved in activation analysis is very straight forward and the technique has been employed for many years.

If a sample containing say N atoms of the nuclear species in question is bombarded, with say neutrons as is done in our case, the activity (A) at any time (t) is given by the following equation:

$$A = N \sigma \phi (1 - e^{-t \ln 2/T_{\frac{1}{2}}})$$

where N = number of nuclei present

σ = cross section of this nuclear species

ϕ = bombarding flux used

$T_{\frac{1}{2}}$ = half life of the nuclear species

As can be seen from the equation and as drawn in Figure V-1 there is a saturation value which is exponentially approached. This saturation value determines the maximum count rate obtained after irradiation and subsequently the accuracy of the concentration measurements attempted, for as is well known high count rates give the best statistics and is the most effective means of minimizing the effect of background. Therefore for a given concentration of a nuclear isotope we obtain best results with (1) a neutron source having the largest possible flux and (2) with those nuclear isotopes which have the largest cross section.

In our work in activation analysis, we simultaneously irradiate two samples containing the same nuclear species in question, one sample being of predetermined concentration and the other sample being our unknown. If we do this and take the ratio of their activities, we see from the above equation that we get,

$$\frac{A_u}{A_s} = \frac{N_u \sigma \phi (1-e^{-t \ln 2/T_{\frac{1}{2}}})}{N_s \sigma \phi (1-e^{-t \ln 2/T_{\frac{1}{2}}})} = \frac{N_u}{N_s}$$

Thus, if we measure the ratio of the activities simultaneously at some time after irradiation and know the number of atoms in our standard sample, we can readily calculate the number of atoms (N_u) in our unknown sample. By knowing the weight of the unknown sample we can then calculate its concentration.

For a neutron source we are presently using an Atomics International L-77 10 watt reactor which gives a neutron flux of approximately 10^8 neutrons per cm^2 per second. This, admittedly, is a low flux and limits our general field of operation. In the very near future, we plan to have a Cockroft-Walton accelerator operational which will give us a flux of approximately 10^9 neutrons/cm^2/sec. We also have at our disposal a large power reactor having a flux of 10^{13} and a cyclotron which enables us to do charged particle irradiations.

To count the activity of our samples we use two 3-inch NaI crystals covered with lead shielding as is shown in Figure V-2. These are connected through amplifiers and single channel analyzers to two scalars as are shown in the console in Figure V-3. Also shown in this figure is a Nuclear Data pulse height analyzer having 4096 channels. This is often used in conjunction with the NaI detectors and also with a Ge(Li) detector to obtain the gamma ray spectrum of our samples.

The procedure followed in making a typical run is the following:

First a Ge(Li) spectrum is taken of the unknown to determine if it is interference free, i.e. to see if it has any other gamma lines other than those originating from the nuclei of interest (vanadium in our case). From this we can determine the need to take steps to correct for any interference present and to determine the optimum settings for our single channel analyzers. If there is no interference from other lines, we can then set the windows on the analyzers to include the gamma Compton envelope as well as the gamma photopeak. This increases our total counts and consequently our statistics. In Figure IV-4, we see a typical NaI spectrum with and without the windows of the single channel analyzers set. In the bottom spectrum of this figure, we see the complete spectrum and in the top spectrum of this figure, we see the same spectrum with the windows set to count just the photopeak and most of the Compton edge of the signal of interest.

Once the above has been determined and the windows set, we then proceed to make a calibration run using a master known (a 2000 ppm sample of vanadium in water for this work) and diluted samples of the same. The latter were samples of concentrations 1000, 400, 100, 50, 10, 5, and 2.5 ppm. A 2000 ppm sample was always simultaneously irradiated and counted with each one of the diluted samples. Thus we know the ratio of atoms in the diluted samples to that of the 2000 ppm samples and by taking the ratio of their count rates and plotting these two things against each other we get the data as drawn in the Figure V-5. As can be seen in this figure, a very straight line was obtained as it should be from the expression derived previously.

This calibration chart gives a measure of the accuracy of the procedure used and allows us to determine the number of nuclei of an unknown without having to know the relative counting efficiencies of the two NaI crystals.

After having made the calibration run, we are then ready to run our unknown. To do this we irradiate simultaneously the unknown along with a standard. We used a 2000 ppm vanadium in distilled water for our standard in the unknown run as well as in the dilution run. After irradiation, we put the samples in our NaI shields and counted their activities simultaneously. By taking the ratio of their activities, and since we know the number of vanadium nuclei in our standard, we can then determine using the calibration curve the number of nuclei of the unknown nuclear species.

In Figure V-6 the results obtained from the residual oil samples furnished by the Laramie Petroleum Center are shown. These samples were taken from the outlet side of the cobalt-molybdate catalyst which had oil in the range of 440 ppm of vanadium going through it. These four samples were taken at four different times ranging over a 10 day period. However, instead of time, the total volume of the residual oil through the catalyst over the volume of the catalyst is plotted on the abscissa. The behavior indicated by the curve drawn through the data points, although admittedly the data points are too few for a decisive conclusion, is characteristic of the operation of catalyst in general and characteristic of the data the chemists at the Laramie Petroleum Center had observed with their sulfur concentrations in the same oil.

In conclusion then, the preliminary data looks encouraging, but many more samples will have to be used and many more runs will have to be made in order to verify the reproducibility of the results and to give us a better idea of the accuracy of our procedure. We have obtained some more samples and are planning on continuing this work.

This work was presented as a paper at the A.A.A.S. meeting in Colorado Springs, Colorado, May 7, 1969. When more samples are analyzed to give better definition to the curve in Figure V-6, a publication is planned for analytical Chemistry.

VI. 37.7 Mev Helium-3 Induced Reactions in Zinc

D. Crisler and H. B. Eldridge, University of Wyoming
C. Zaidins, University of Colorado

INTRODUCTION:

In an attempt to understand nuclear reactions at excitation energies much larger than the average binding energy per nucleon, the concept of the compound nucleus has proven to be quite useful. The basic assumption is that an external particle which strikes a nucleus will rapidly share its energy with all the nucleons in the struck nucleus. Consequently, a relatively long time evolves before a single nucleon in the "compound nucleus" can acquire enough energy to escape. Thus, as has been verified experimentally, one would expect that the decay of a compound nucleus should be independent of its mode of formation.

The cross-section for the decay of a compound nucleus found in channel α of excitation energy E into an exit (decay) channel β may be written as:

$$\sigma_{\alpha\beta}(E) = \frac{\sigma_\alpha \Gamma_\beta}{\Gamma}$$

where σ_α = cross-section for formation of compound nucleus in entrance channel α,

$\frac{\Gamma_\beta}{\Gamma}$ = relative probability for decay of the compound nucleus into channel β and Γ is sum of all possible decay modes.

The relative probability of decay into a given channel can be written in terms of the cross-sections for formation

$$\frac{\Gamma_\beta}{\Gamma} = \frac{k_\beta^2 \sigma_\beta}{\sum_i k_i^2 \sigma_i}$$

where k_i is the wave number of channel i which gives the same excitation energy to the compound system, and we sum over all possible i.

We have initiated a program within the Accelerator Laboratory at the University of Wyoming in collaboration with the Nulcear Physics Laboratory at the

University of Colorado to deduce the relative probabilities for decay of a given compound nucleus by measuring the radioactivity in the target after bombardment. We are currently in the process of measuring $\sigma_{\alpha\beta}(E)$ for a range of different compound nuclei versus a range of excitation energies. With our modern high resolution gamma ray spectroscopy system we believe we can measure $\sigma_{\alpha\beta}(E)$ for several values of β at the same time without having to perform radiochemical separation of the target after bombardment.

EXPERIMENTAL SET-UP:

An enriched Zn^{64} target of approximately 30 mg is placed in a holder as shown in Figure VI-1. The target holder is water-cooled with cold water in direct contact with the target backing plate. The beam of He^3 particles from the cyclotron is adjusted to get maximum current of 3.8μamp on the target. As shown in Figure VI-1 the current in measured off the graphite collimator and the holder, both of which are isolated from ground. The beam is adjusted until the collimator current is a minimum and the holder current a maximum.

After the target had been bombarded for 6.75 hours, it was taken from the holder and allowed to decay from ∿ 100 R/h at 1 ft to ∿ 3 R/hr at contact after which time it was flown to the University of Wyoming where gamma spectra covering the energy range of 0-4 Mev were taken as a function of time.

The equipment used at the University of Wyoming consists of a 2cc Ge(Li) diode, preamplifier, linear amplifier, and 4096 channel PHA. See Figure VI-2.

EXPERIMENTAL PROCEDURE:

Although we did not calibrate our Ge(Li) detectors for absolute efficiency versus photopeak energy, we were able to get a "secondary" calibration by comparing the measured relative efficiency of our detector versus published data on absolute efficiencies of Ge(Li) detectors of different sensitive volumes. See Figure VI-3.

As the spectra were being accumulated clock time as well as live time of the PHA were recorded to allow later corrections. After a spectrum had been accumulated, the memory contents of the PHA were punched on paper tape. The paper tape was then read into the computer, interpreted, and stored on magnetic tape. By a computer program, the entire 4096 channel spectrum is plotted out, 100 channels per page. See Figure VI-4. By scanning these plots, the relevant peak centroids are easily ascertained, and then by a second computer program, the

position of these peaks are fitted with a background subtraction (Figure VI-5) from which the computer tabulates the net areas as a function of time, makes a plot of the logarithum of the area versus time, and then computes the half-life and disintegration rate for each peak for the time at the end of the bombardment of the target.

RESULTS:

From the energy and half-life of each gamma line, the identification of various isotopes was possible. See Figure VI-6. The two main constituents of our target, Zn^{64} and Zn^{66}, gives us these reactions

$$He^3 + Zn^{64} \rightarrow Ge^{67*}$$

$$He^3 + Zn^{66} \rightarrow Ge^{69*}$$

from which these compound nuclei can decay by emission of neutrons, protons, or other particles. Theoretical calculations made by Stuart Ahrens of our laboratory reveal that isotopes of mass 64 or 65 can result only from the decay of Ge^{67*} and isotopes of mass 66 or 67 can result only from the decay of Ge^{69*}. These calculations were for 3 particle emissions of neutrons and/or protons only, and presently he is working on 4 particle emissions of neutrons and/or protons as well as He^3 and He^4 particle emissions.

With a knowledge of the initial disintegration rate and the relative gamma intensity of each line, one can determine the cross section for formation of each isotope present in the target. Relative yields of identified isotopes are shown in Figure VI-7. If we use the 1039 Kev line of Ga^{66} as the standard and compare all yields relative to it, we get the value shown in the figure.

CONCLUSION:

The results obtained indicate that we can successfully measure the relative yields for the various isotopes produced by this method. Some other isotopes yet to be identified will give us additional information about yields and cross sections for decay into a specified channel for several values of β.

This work was presented as a paper at the A.A.A.S. meeting in Colorado Springs, Colorado, May 7, 1969.

VII. Neutrons from Heavy Ion Bombardment

W. G. Simon and S. T. Ahrens
University of Wyoming

We have examined in detail the effects of transfer reactions from heavy ion bombardment on the emitted particle spectra. According to recent measurements[1,2] a large fraction of the total reaction cross section consists of transfer reactions. We assume that the transferred part of the heavy ion plus the target nucleus form a compound system which then emits particles according to the statistical model. There is some evidence for this assumption in the observations of Phohl.[2] Owing to the forward momentum of the non-transferred particle this compound system moves backward in the center-of-mass system. We have incorporated a multiple particle evaporation computer code, which includes the effects of angular momentum to calculate the effects of transfer reactions on the particle spectra. Some general features of the spectra are: 1) a "softening" of the spectra resulting from lower average excitation energies; 2) a backward peaking of particles at most energies which results from the backward motion of the evaporating system; 3) charged particles appear in the center-of-mass system well below the Coulomb barrier for compound nucleus reactions and these are forward peaked in the c.m.s. This latter result can be understood if we consider that particles emitted near the barrier in the compound system will appear at still lower energies in the center-of-mass system if emitted in the forward direction. Thus we add still one more explanation to the long list of reasons[3] given for the observation of particles emitted well below the Coulomb barrier in reactions. This cannot account for all cases since such emission is observed for proton bombardment where the explanation does not apply.

The results of these calculations have been compared with our own neutron measurements and with the results of Knox et. al. for charged particle spectra. The calculations are in reasonable qualitative agreement with experiment. We emphasize that no adjustable parameters were used. For the case of neutrons, the softening of the spectra and the backward peaking are very definite in the observed spectra. For the case of charged particles the expected features are not so clear in the observed spectra, although there is no clear disagreement. We interpret the 16 MeV alpha particle, (see Figure VII-1) angular distribution to be the result of a backward peaked evaporation spectrum plus a forward direct reaction peak. Someone else may interpret this to be a nearly symmetric angular distribution resulting from compound nuclear interactions. However, the dip

at 90^{o} is much deeper than any angular momentum calculations would indicate. Similarly for alphas at 8 MeV, owing to the lack of information at backward angles, there is some question whether the particles are forward peaked as predicted by the calculations.

The penetration factors used in this analysis, based on the Hill-Wheeler formula, are probably inaccurate enough to affect the results. We are replacing these by "back nucleus" penetration factors.

References

(1) L. Kowalski, J. C. Jodogne and J. M. Miller, Phys. Rev. 169, 894 (1968).

(2) Raymond Pfohl, "Reactions Nucleaires Provoquees Par Les Interactions Du^{20}Ne De 200 MeV Avec Les Noyaux De L'Emulsion Ionographique", De L'Universite De Strasbourg, thesis (unpublished).

(3) J. R. Grover and J. Gilet, Phys. Rev. 157, 823 (1966).

VIII. Calculation of Excitation Functions

S. T. Ahrens, University of Wyoming

In conjunction with the experimental work on the excitation functions for He^{3} on Zn^{64} and Zn^{66}, a calculation adapted from West[1] has been used. Basically this program gives the probability of ending up with a given Z and N, providing the projectile and target form a compound nucleus.

The program has been adapted from West's original program in the following way. First, instead of considering only the case where three nucleon emission is possible, the program is now capable of handling excitation energies where from one to four nucleons are emitted. Secondly, the form of the output has been changed to give relative yields as a function of Z and N, instead of the spectra of emitted particles. Lastly, the pairing energies of Cameron[2] have been replaced by those of Seeger.[3]

The major limitations of this analysis can be stated as (a) a complete neglect of other than nucleon emission and (b) a complete neglect of angular momentu The next version of this calculation, which is being written up now, will overcome these limitations.

A typical output is shown in Figure VIII-1. Each square corresponds to a given value of Z and N, the arrangement of the squares being the same as on the Chart of the Nuclides. Within each square there are three numbers. If we

assume that we have formed 10,000 compound nuclei (upper right square), then the three numbers per box can be read as follows: "In", refers to the number of times that the particular isotope of interest has been formed during the evaporation process; "Out", refers to the number of times that the isotope of interest has been formed and then undergoes further nucleon evaporation; and "Left", refers to the number of times that the isotope of interest has been formed, but does not evaporate off any further nucleons. It is this latter category that is of primary interest in excitation function work. Thus if one forms 10,000 Ge67 compound nuclei with 37.7 MeV He3 on Zn64, one should end up with 0 Ge66's, 2 Ge65's, 24 Ga65's, etc.

A summary of the excitation function for He^3 on Zn64 and Zn66 is shown in tabular form in figures VIII-2 and VIII-3. Again all numbers have been normalized to 10,000.

References

(1) West, R. W., Proton Emission in 42-MeV Alpha Particle Bombardment of Several Elements (Doctoral thesis, University of Washington, SEattle, Washington, (1963).
(2) Cameron, A. B., Can. J. Phys. 36, 1040 (1958).
(3) Seeger, P.A., Nuclear Physics 25, 1 (1961).

IX. Neutron Spectra from Charged Particle Reactions

W. G. Simon, S. T. Ahrens, H. B. Eldridge, University of Wyoming
D. Lind, University of Colorado

The neutron spectra from the following four reactions,

(1) 26.0 MeV Protons on Ni^{60}
(2) 26.0 MeV Protons on Cu^{63}
(3) 31.3 MeV Alphas on Ni^{60}
(4) 31.3 MeV Alphas on Cu^{63}

have been obtained and are shown in Figures IX-1, IX-2, IX-3, IX-4. While these four reactions have at least one parameter in common with one another, reactions (1) and (3) both yield the same compound nucleus at the same excitation energy, but with different average angular momenta.

The following observations can be made:

(1) At low energies (4 MeV and below) all of the reactions are nearly symmetric about 90^0. It is thus believed that these are compound nucleus neutrons.

(2) At higher energies (4 MeV and above) all of the reactions (except no. 1) show a forward peaking which increases with neutron energy. It is believed that the asymmetry is due to a contribution from direct reaction neutrons.

(3) At low energies (4 MeV and below) the proton induced reactions (1) and (2) are much flatter than the alpha induced reactions (3) and (4). This difference is attributed to the different angular momentum which the proton and alpha induced reactions have. Reactions (2) and (3), as mentioned earlier, differ only in their average angular momenta, and thus they will be used in making a quantitative study of the role of angular momenta in compound nuclear reactions.

(4) Lastly, although there is some question about the reliability of the absolute value of the total cross sections, there is a noticeable increase in total cross-section as one goes from reactions (1) to (4). It is to be noted that this is consistent with the trend of the geometric cross-sections.

This work was presented as a paper at the A.A.A.S. meeting in Colorado Springs, Colorado, May 7, 1969.

X. Charged Particle Spectra from Charged Particle Reactions
S. T. Ahrens, W. G. Simon, H. B. Eldridge, University of Wyoming

To complement the neutron spectra obtained from the four reactions listed in section IX, we are preparing to measure the charged particle spectra for these same four reactions. The charged particles of interest are the proton, deuteron, triton, helium-3, and helium-4. It is hoped that we will be able to identify and record energies down to 2 MeV for the Z = 1 particles, and 8 MeV for the Z = 2 particles.

The charged particle spectrometer to be used is shown in Figure X-1. It is the Particle Identifier Output (P.I.O.) which is of main importance here, and its resolution is largely dependent on the thickness of the ΔE detector.

Tables X-2, X-3, X-4, X-5 shows the effect of the thickness of the ΔE detector on the P.I.O. for the particles types and energies mentioned earlier. Thus if one ignores all noise, and 20μ detector gives the best resolution for our experiment.

Currently, this calculation is being expanded to take account of noise in the detector, preamplifiers, and amplifiers. We suspect that this will show that the optimum thickness will be greater than 20μ.

(2) At higher energies (4 MeV and above) all of the reactions (except no. 1) show a forward peaking which increases with neutron energy. It is believed that the asymmetry is due to a contribution from direct reaction neutrons.

(3) At low energies (4 MeV and below) the proton induced reactions (1) and (2) are much flatter than the alpha induced reactions (3) and (4). This difference is attributed to the different angular momentum which the proton and alpha induced reactions have. Reactions (2) and (3), as mentioned earlier, differ only in their average angular momenta, and thus they will be used in making a quantitative study of the role of angular momenta in compound nuclear reactions.

(4) Lastly, although there is some question about the reliability of the absolute value of the total cross sections, there is a noticeable increase in total cross-section as one goes from reactions (1) to (4). It is to be noted that this is consistent with the trend of the geometric cross-sections.

This work was presented as a paper at the A.A.A.S. meeting in Colorado Springs, Colorado, May 7, 1969.

X. Charged Particle Spectra from Charged Particle Reactions

S. T. Ahrens, W. G. Simon, H. B. Eldridge, University of Wyoming

To complement the neutron spectra obtained from the four reactions listed in section IX, we are preparing to measure the charged particle spectra for these same four reactions. The charged particles of interest are the proton, deuteron, triton, helium-3, and helium-4. It is hoped that we will be able to identify and record energies down to 2 MeV for the Z = 1 particles, and 8 MeV for the Z = 2 particles.

The charged particle spectrometer to be used is shown in Figure X-1. It is the Particle Identifier Output (P.I.O.) which is of main importance here, and its resolution is largely dependent on the thickness of the ΔE detector.

Tables X-2, X-3, X-4, X-5 shows the effect of the thickness of the ΔE detector on the P.I.O. for the particles types and energies mentioned earlier. Thus if one ignores all noise, and 20μ detector gives the best resolution for our experiment.

Currently, this calculation is being expanded to take account of noise in the detector, preamplifiers, and amplifiers. We suspect that this will show that the optimum thickness will be greater than 20μ.

APPENDIX

The following is a list of papers and publications supported in part by Contract AT(11-1)-1549.

COO-1549-09 Fast Neutron Dose from a PuBe Source
R. A. Shader, H. B. Eldridge
Health Physics 16 #6 (1969)

COO-1549-10 RENEWAL PROPOSAL TECHNICAL PROGRESS REPORT 1968

COO-1549-11 37.7 Mev Helium-3 Induced Reactions in Zinc
D. Crisler, L. J. Detch, Jr., W. G. Simon, and H. B. Eldridge, R. S. Dingus and C. S. Zaidins
Paper presented at the Physical Sciences Section Southwestern and Rocky Mountain Division American Association for the Advancement of Science and Colorado-Wyoming Academy of Science, Colorado Springs, Colorado, May 7-10, 1969.

COO-1549-12 Measured Efficiency of a Ge(Li) Detector
J. Jarmer and H. B. Eldridge
Paper presented at the Physical Sciences Section Southwestern and Rocky Mountain Division American Association for the Advancement of Science and Colorado-Wyoming Academy of Science, Colorado Springs, Colorado, May 7-10, 1969.

COO-1549-13 Activation Analysis of Trace Metals in Oil
John P. Flaherty and H. B. Eldridge
Paper presented at the Physical Sciences Section Southwestern and Rocky Mountain Division American Association for the Advancement of Science and Colorado-Wyoming Academy of Science, Colorado Springs, Colorado, May 7-10, 1969.

COO-1549-14 Study of Particles Emitted from Zn^{64} Compound Nuclei Formed in Two Ways: $P + Cu^{63}$ and $\alpha + Ni^{60}$.
S. T. Ahrens, W. G. Simon, and H. B. Eldridge
Paper presented at the Physical Sciences Section Southwestern and Rocky Mountain Division American Association for the Advancement of Science and Colorado-Wyoming Academy of Science, Colorado Springs, Colorado, May 7-10, 1969

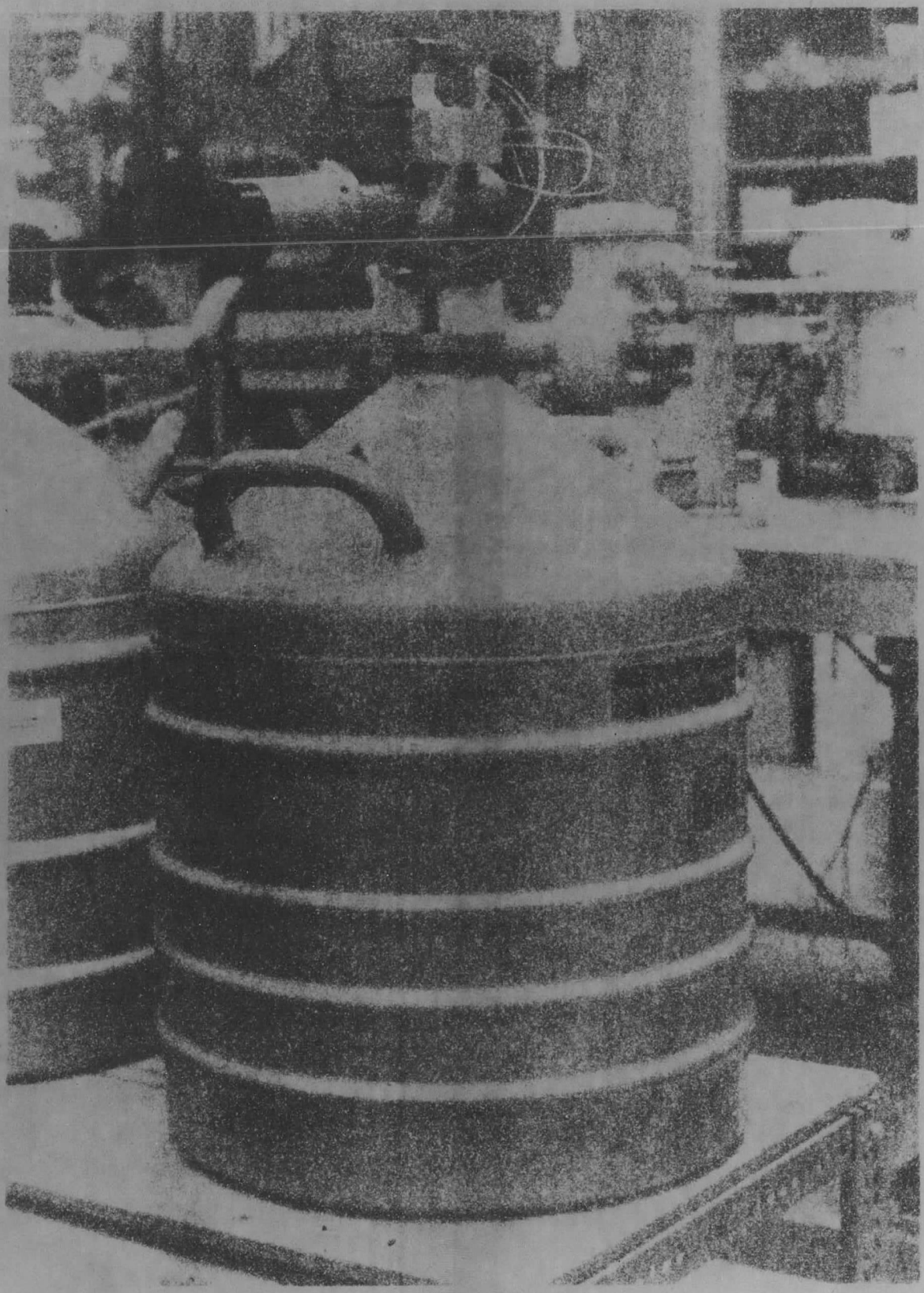

Fig IV-1

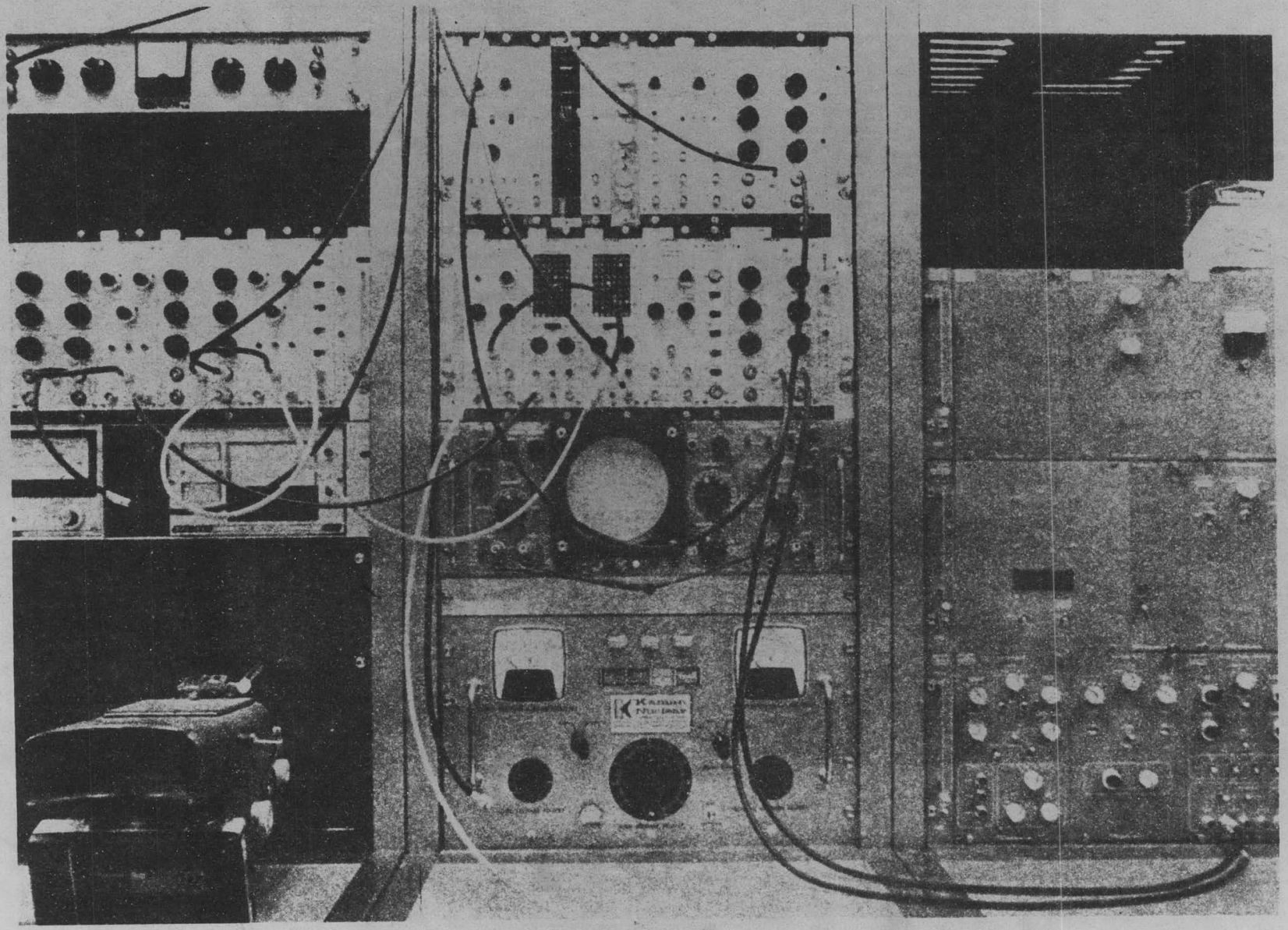

Fig IV-2

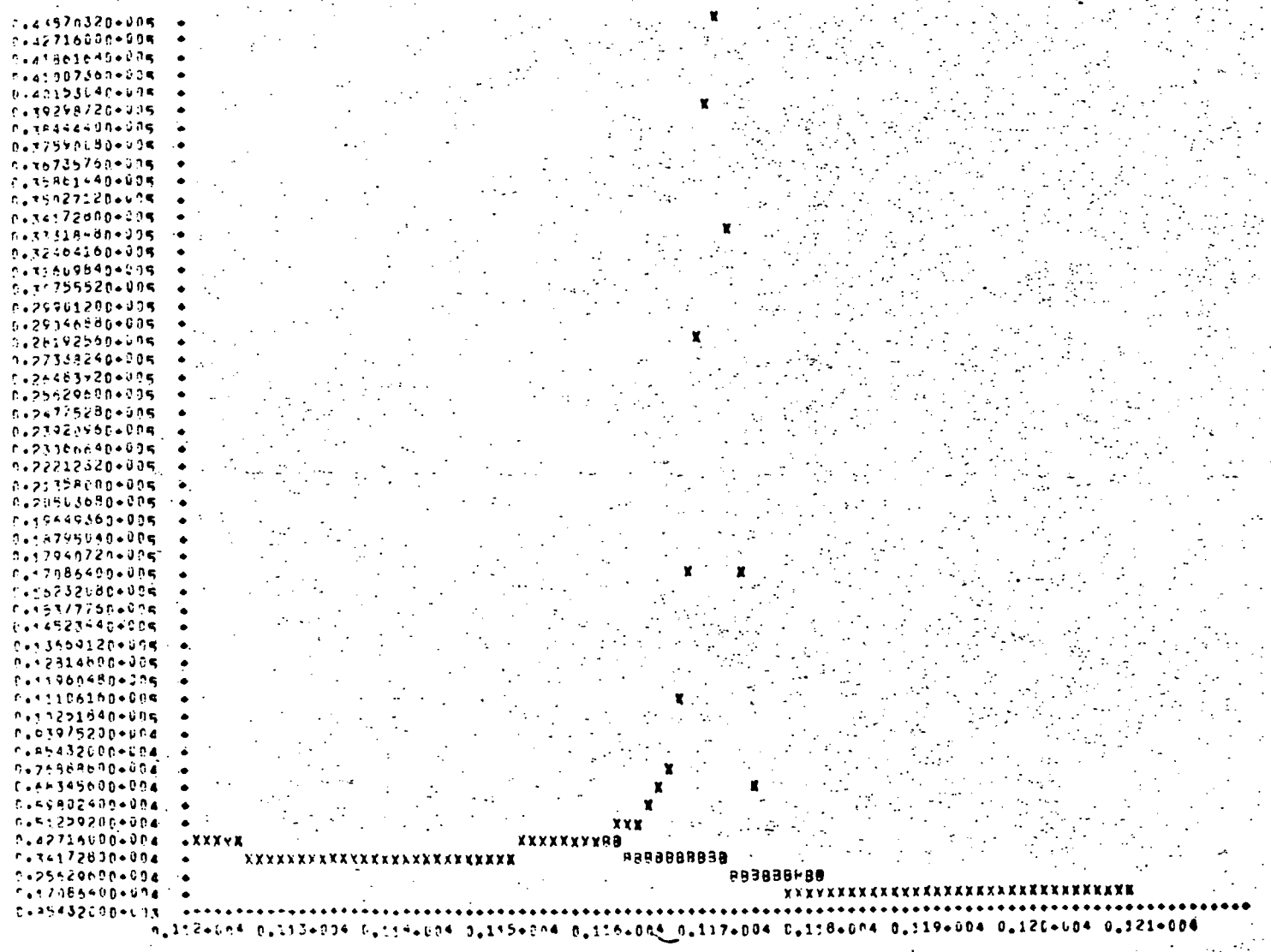
0.117E+004 0.118E+004 0.119E+004 0.120E+004 0.121E+004
0.475473E+002 COUNTS/SEC. PEAK 117;RUN LUMA 48 EFFICIENCY MEASUREMENT RYAN 4.5CC ORTEC C060 4 7 69

Fig IV-3

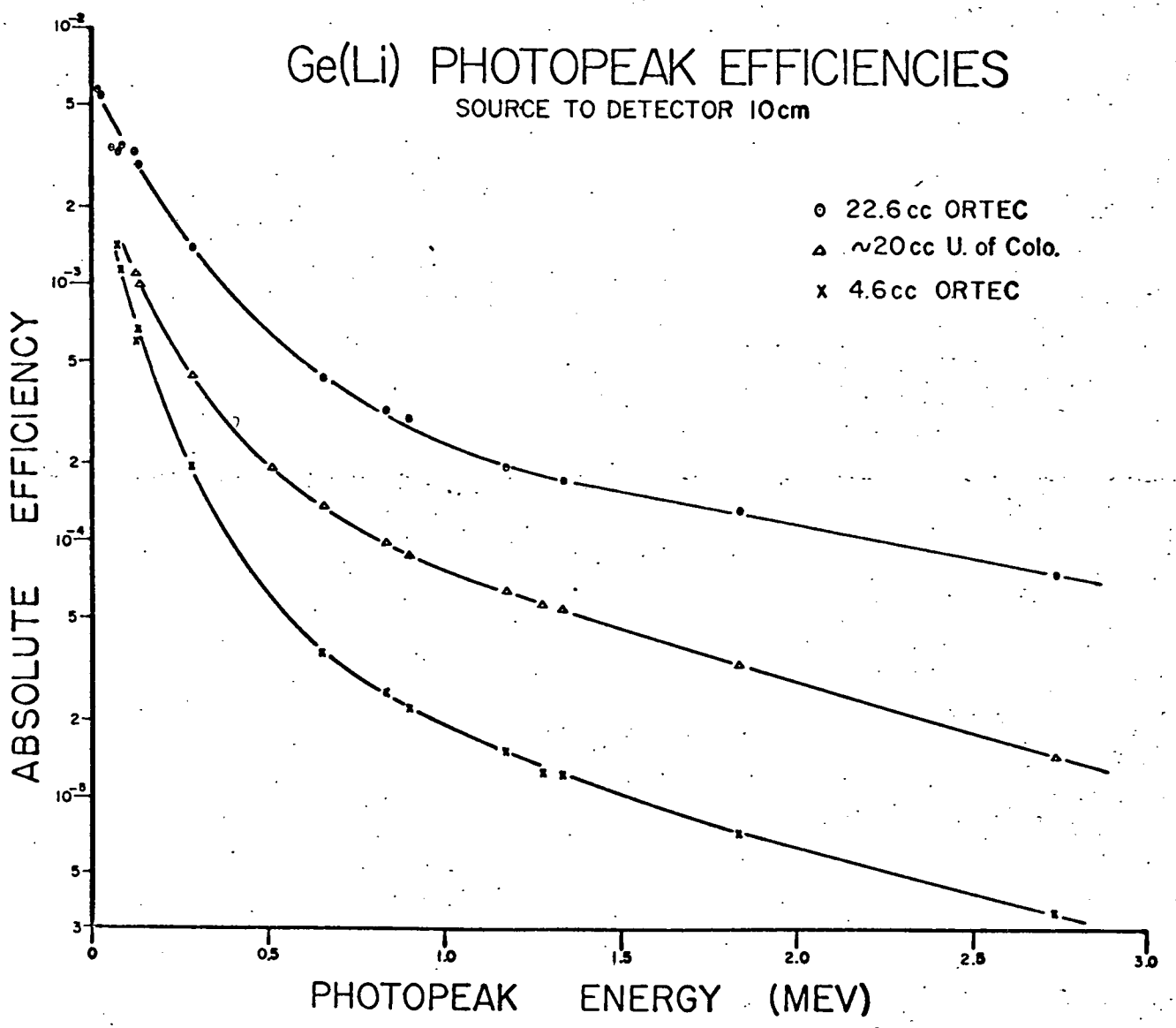
Ge(Li) PHOTOPEAK EFFICIENCIES
SOURCE TO DETECTOR 10cm
o 22.6cc ORTEC
Δ ~20cc U. of Colo.
x 4.6cc ORTEC
ABSOLUTE EFFICIENCY
PHOTOPEAK ENERGY (MEV)
0
0.5
1.0
1.5
2.0
2.5
3.0

Fig IV-4

$$A = N\sigma\Phi(1-e^{-t\ \ln 2/T_{1/2}})$$

where

A = activity (dN/dt)

σ = cross section

Φ = flux

$T_{1/2}$ = half-life

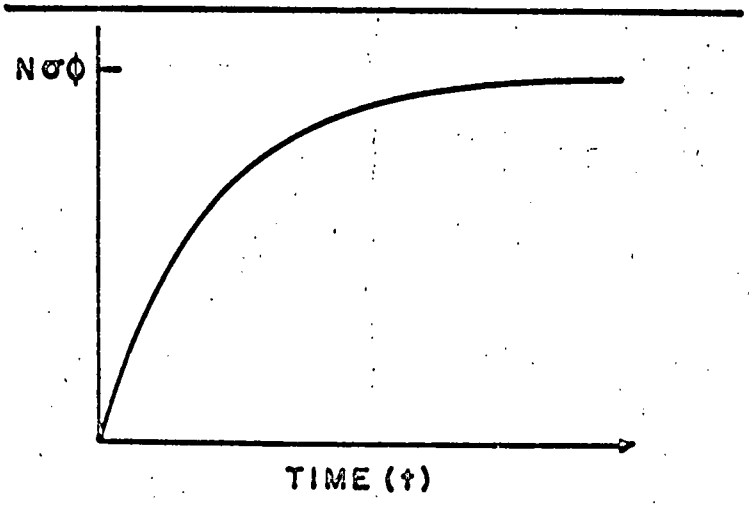

Fig V-1

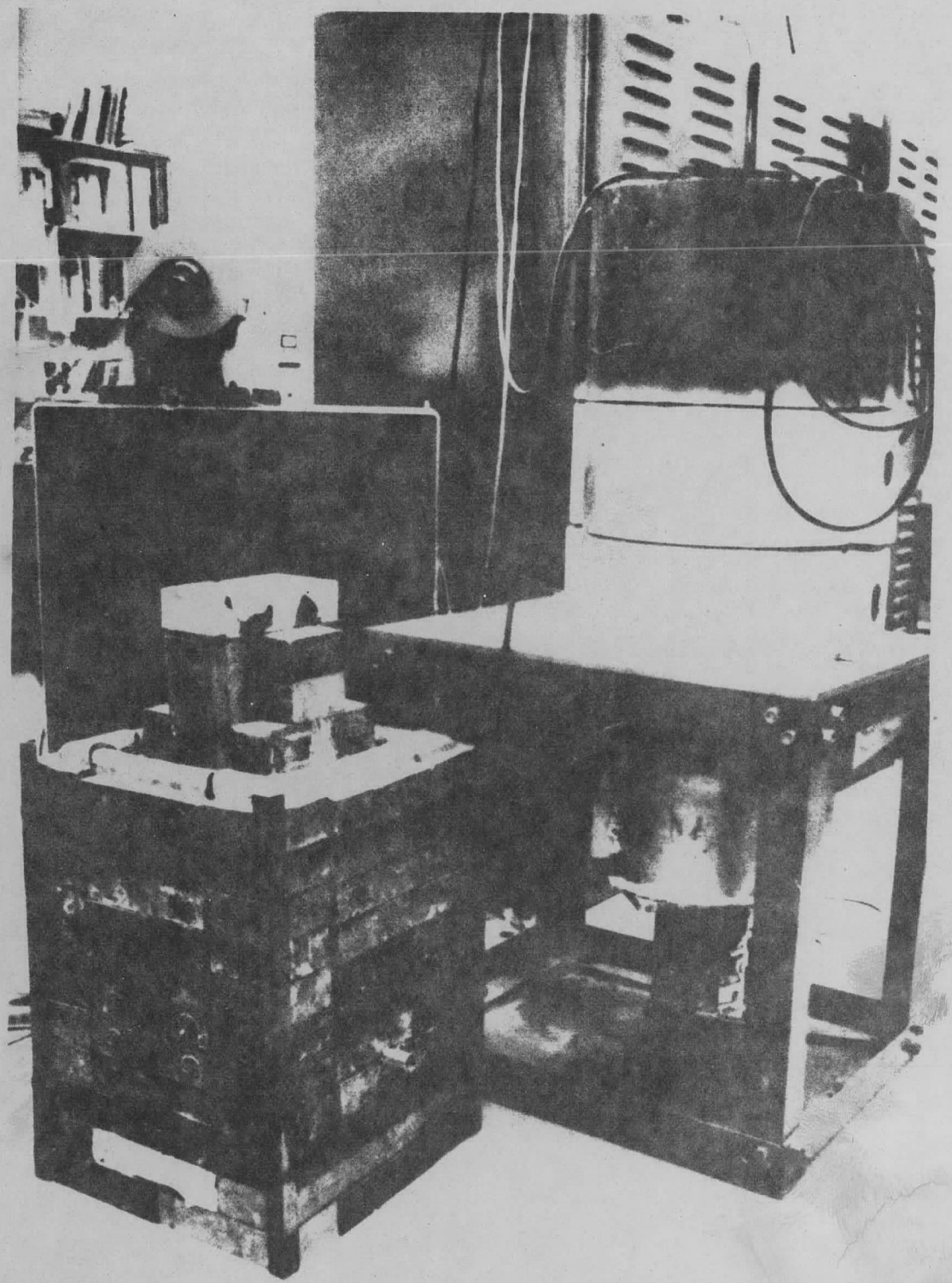

Fig V-2

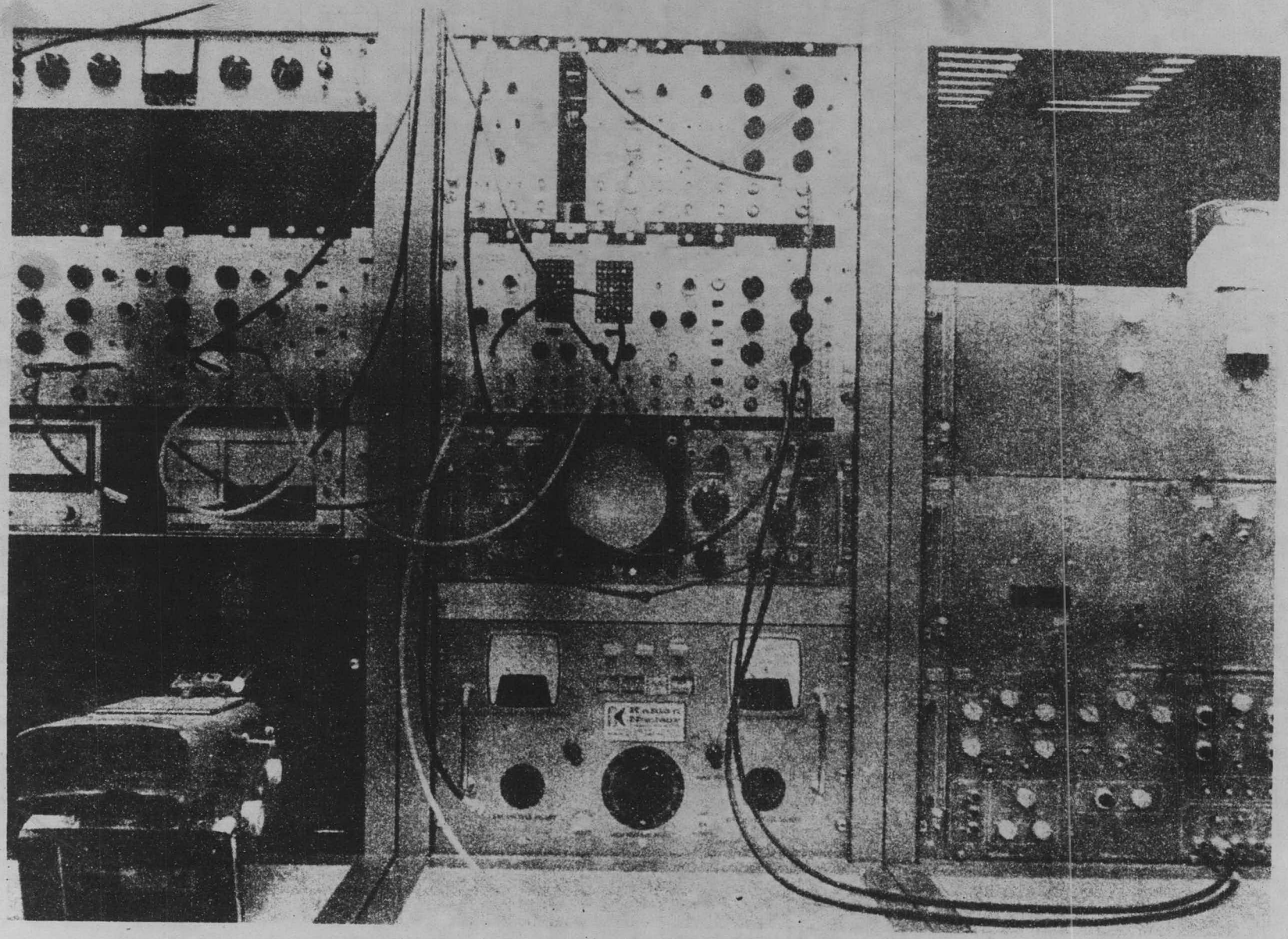

Fig V-3

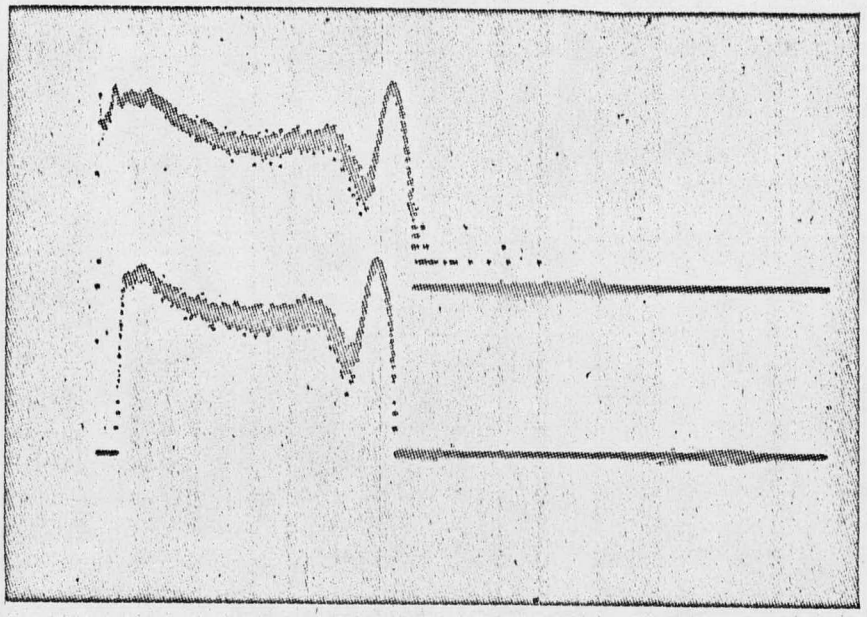

Fig V-4

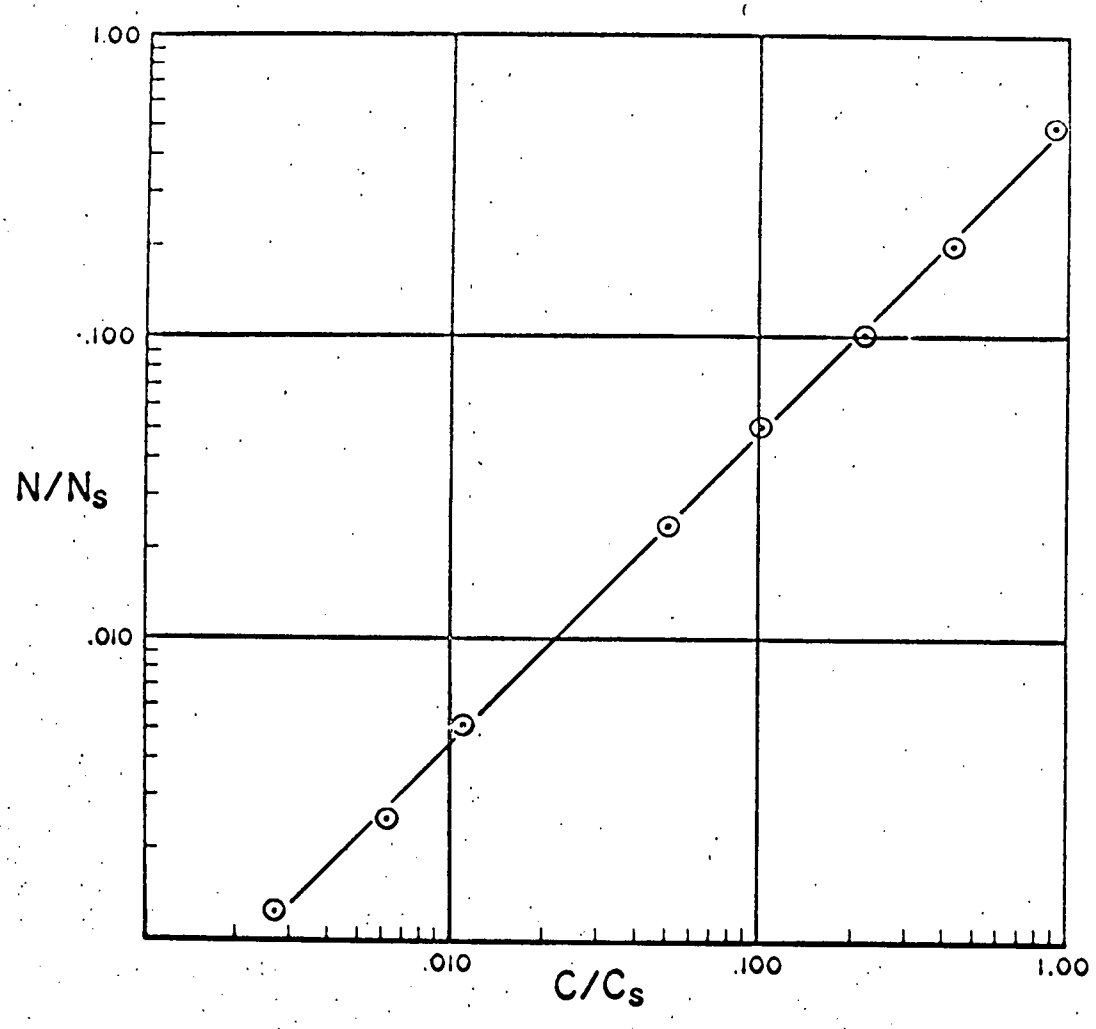

Fig V-5

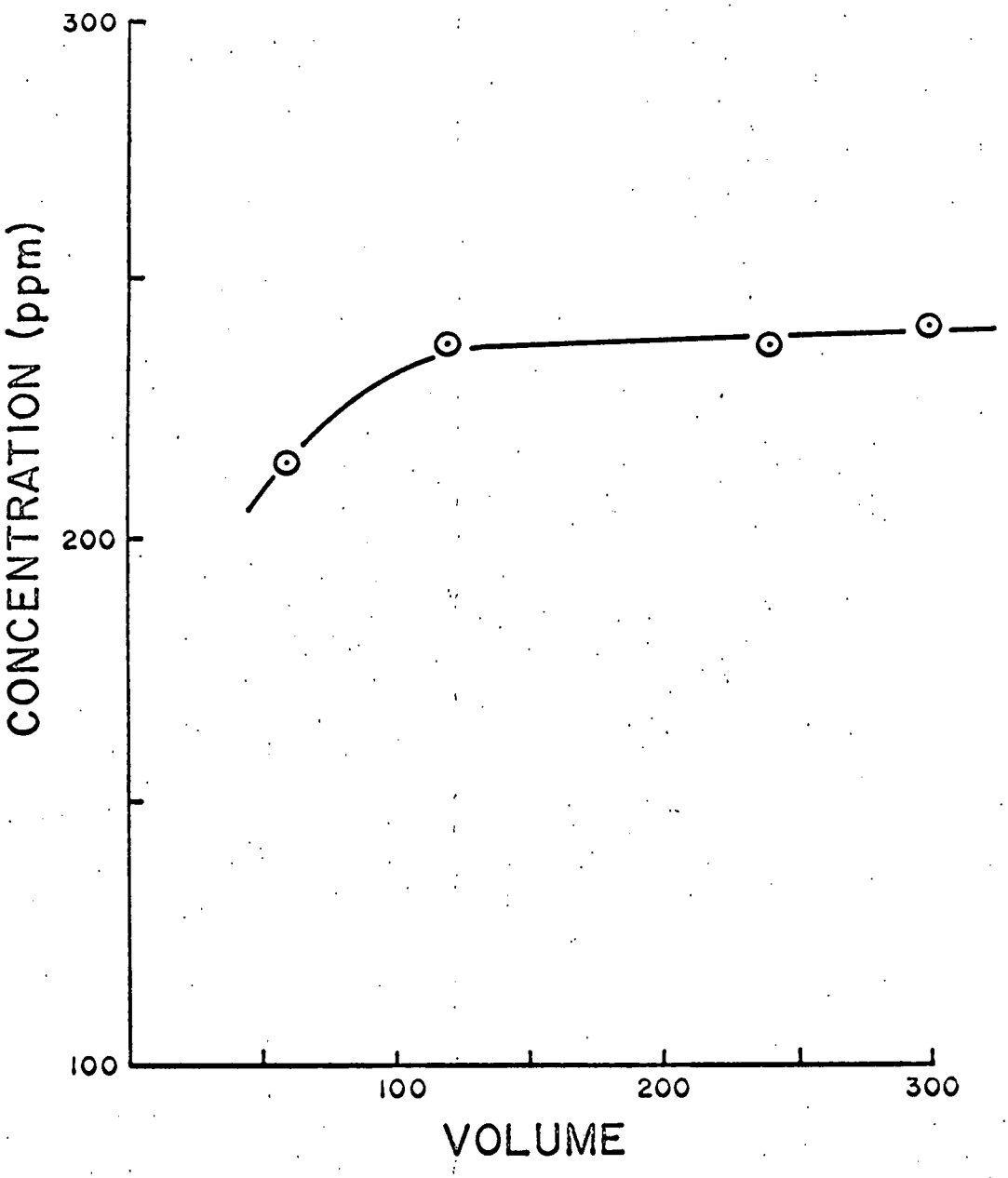

Fig V-6

TARGET ASSEMBLY

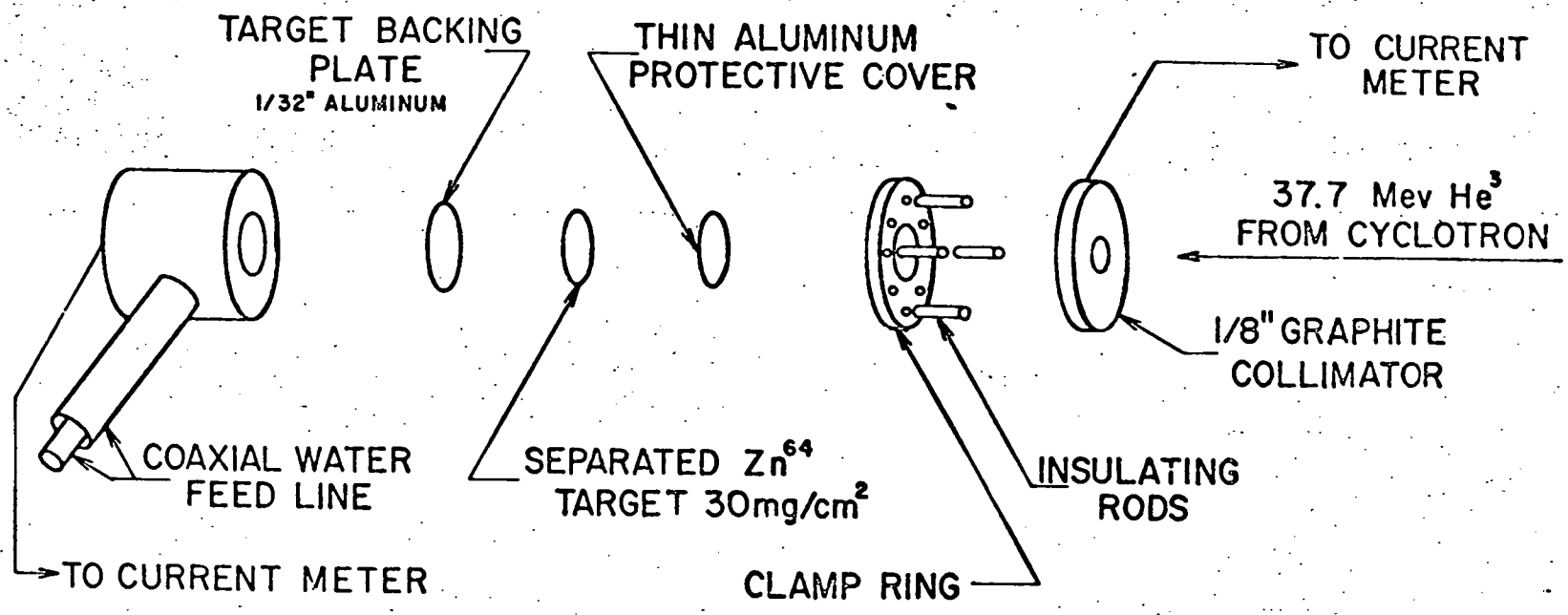

Fig VI-1

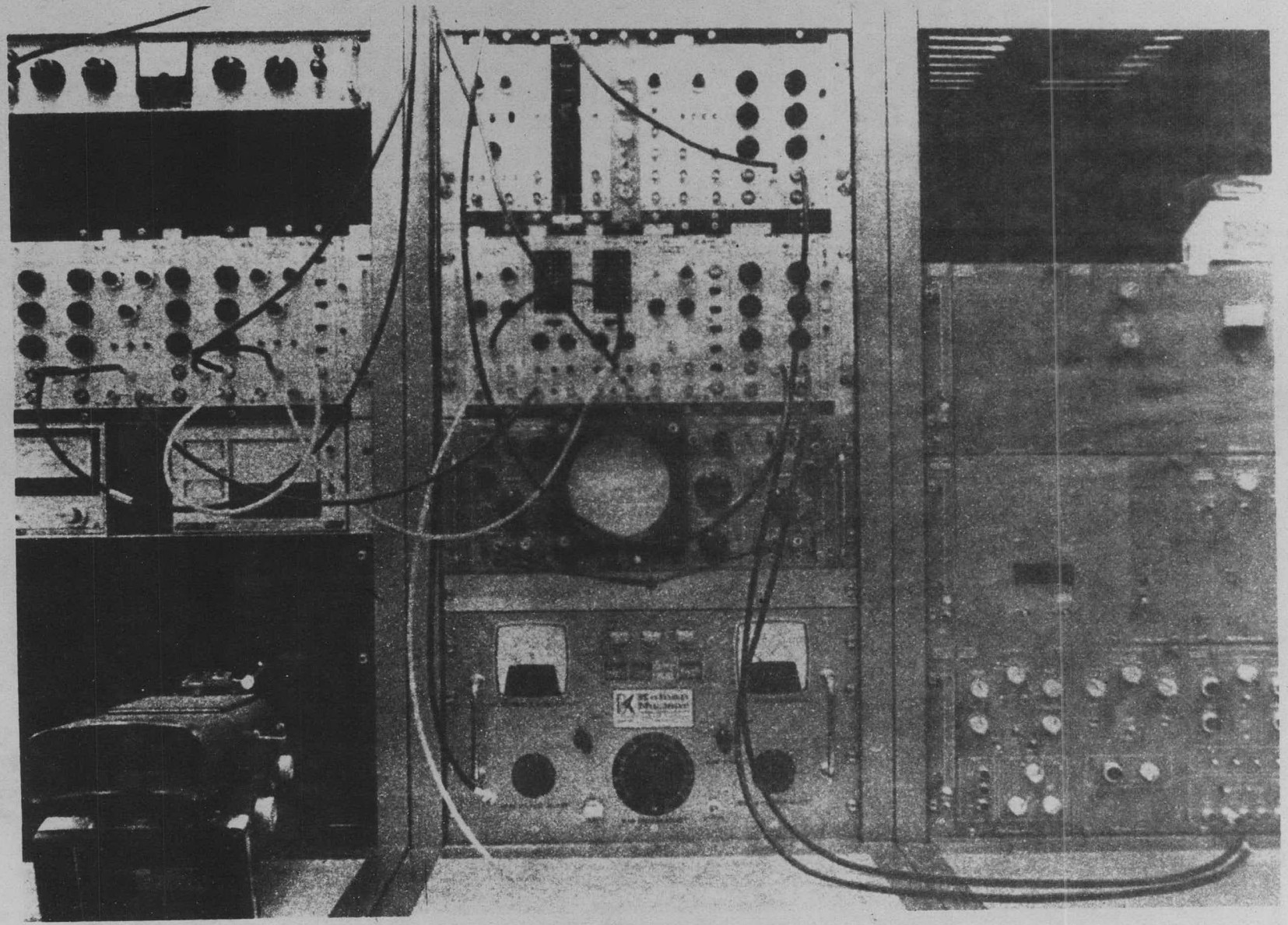

Fig VI-2

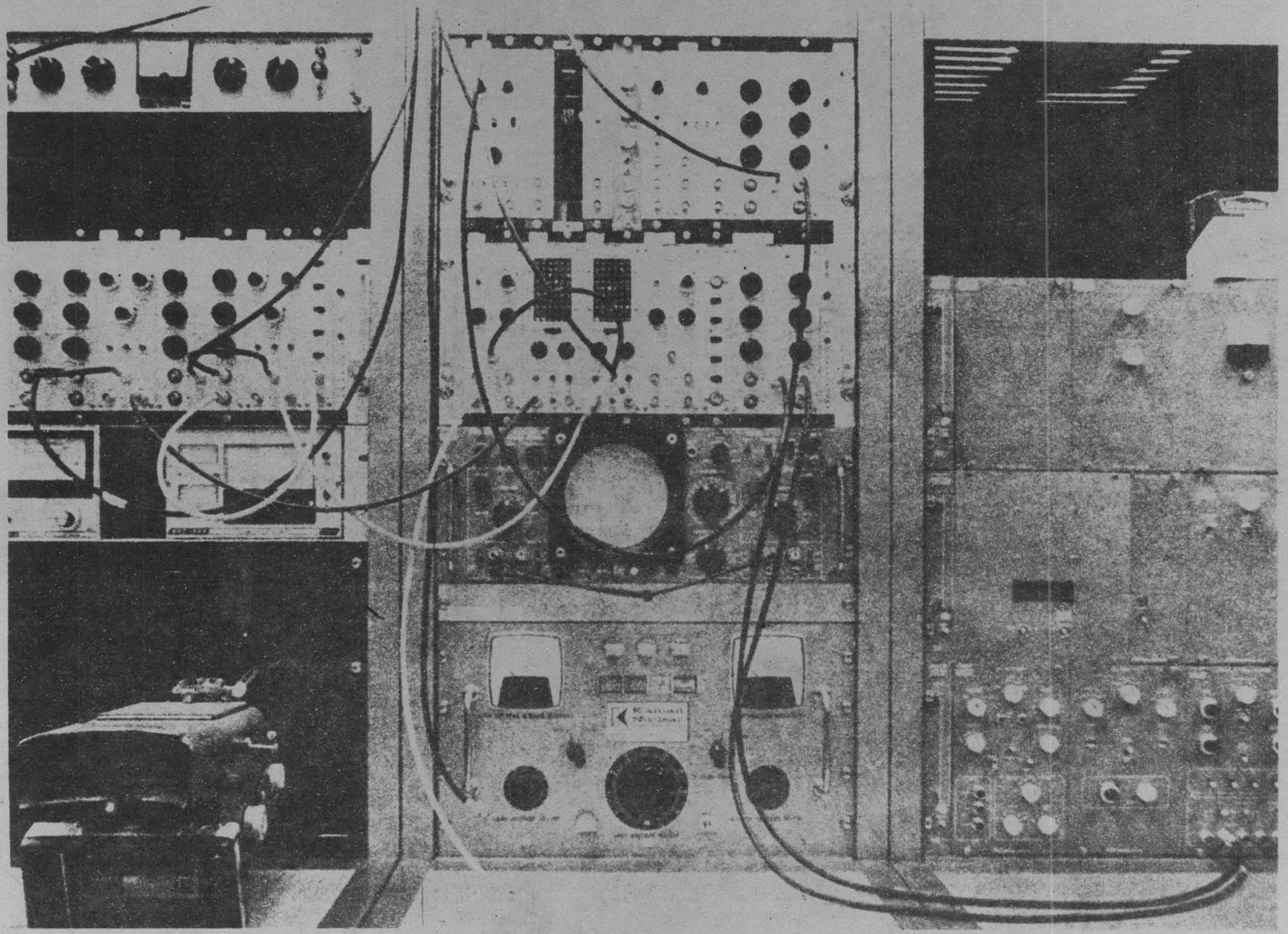

Fig VI-2

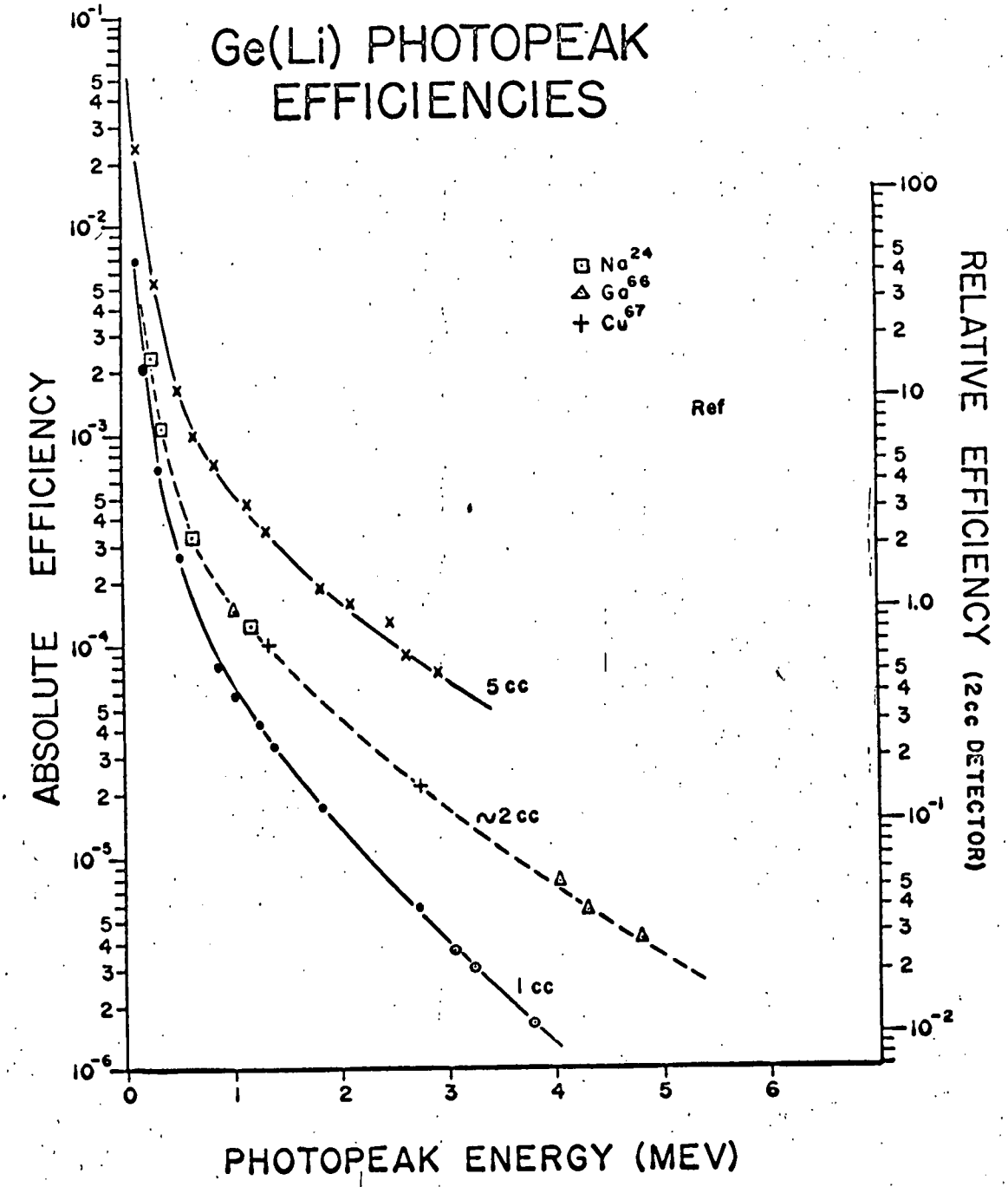
Ge(Li) PHOTOPEAK EFFICIENCIES
ABSOLUTE EFFICIENCY
RELATIVE EFFICIENCY (2cc DETECTOR)
PHOTOPEAK ENERGY (MEV)
Na24
Ga66
Cu67
Ref
5 cc
~2 cc
1 cc

Fig VI-3

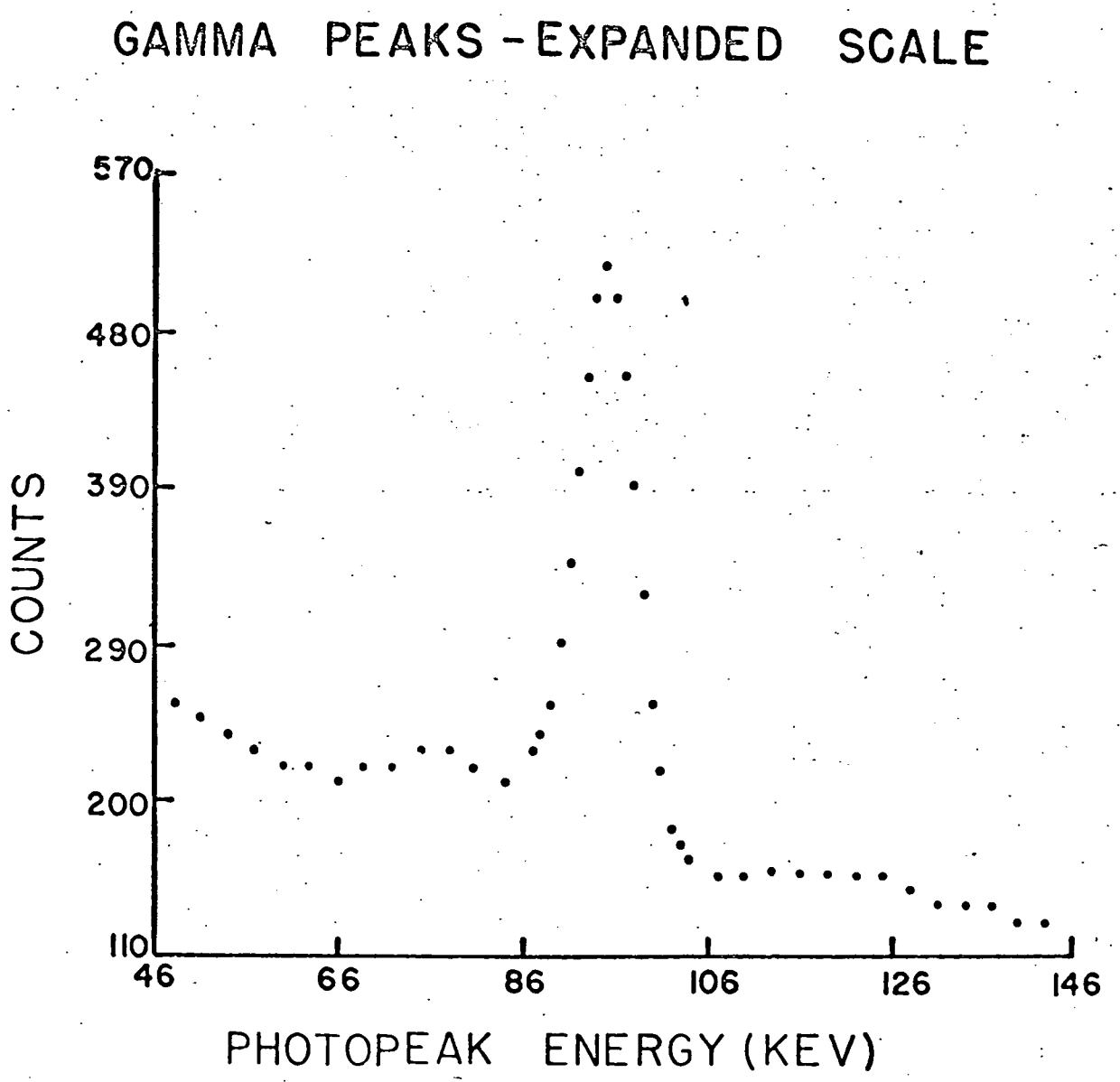
GAMMA PEAKS - EXPANDED SCALE
570
480
390
290
200
110
COUNTS
46
66
86
106
126
146
PHOTOPEAK ENERGY (KEV)

Fig VI-4

BACKGROUND SUBTRACTION FROM GAMMA PEAKS

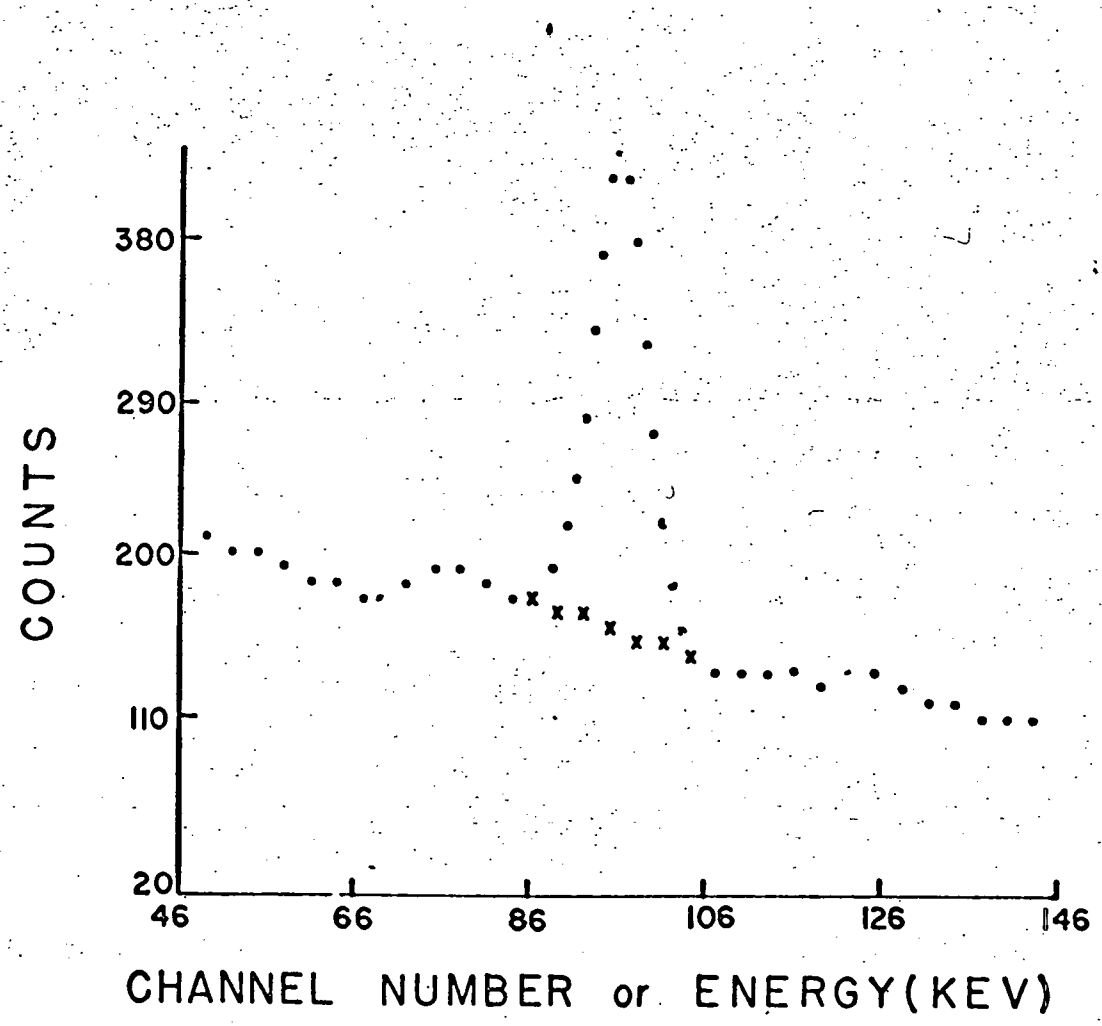

Fig VI-5

ISOTOPES PRODUCED IN ZINC BOMBARDMENT

WITH 37.7 MEV He^3 IONS

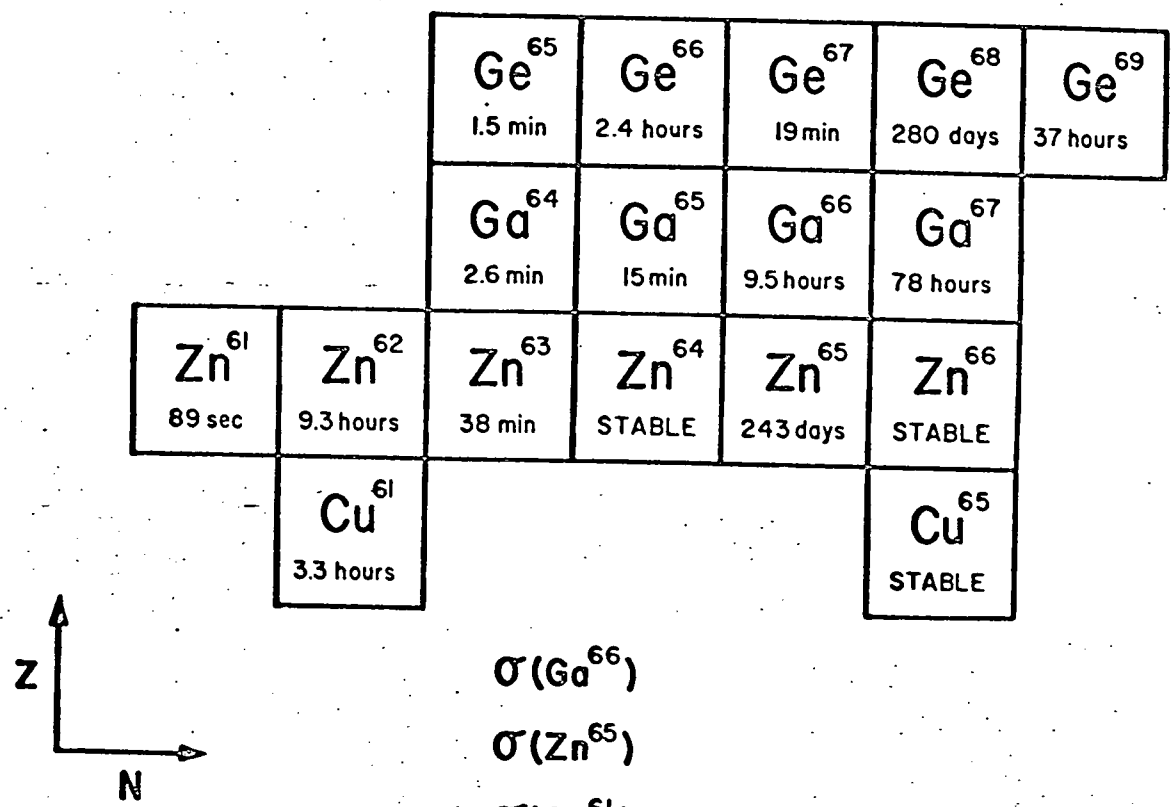

Fig VI-6

RELATIVE YIELDS

He^3 + Zinc at 37.7 Mev

ISOTOPE	$T_{1/2}$	GAMMA ENERGY (kev)	GAMMA INTENSITY	RELATIVE YIELD	AVERAGE
Ga^{66}	9.5 hr	1039	.390	1.00	1.02
		4086†	.011	1.11	
		4295†	.036	0.95	
		4806†	.016	1.02	
Ga^{67}	78.1 hr	96	.700	2.67	3.47
		185	.207	4.27	
Cu^{61}	3.3 hr	285	.130	8.42	7.72
		374	.019	6.78	
		656	.096	7.90	
		1185	.036	7.76	
Zn^{65}	243.8 d	1115	.506	20.42	20.42

† The double escape peak of these lines was observed.

Fig VI-7

Fig VII-1

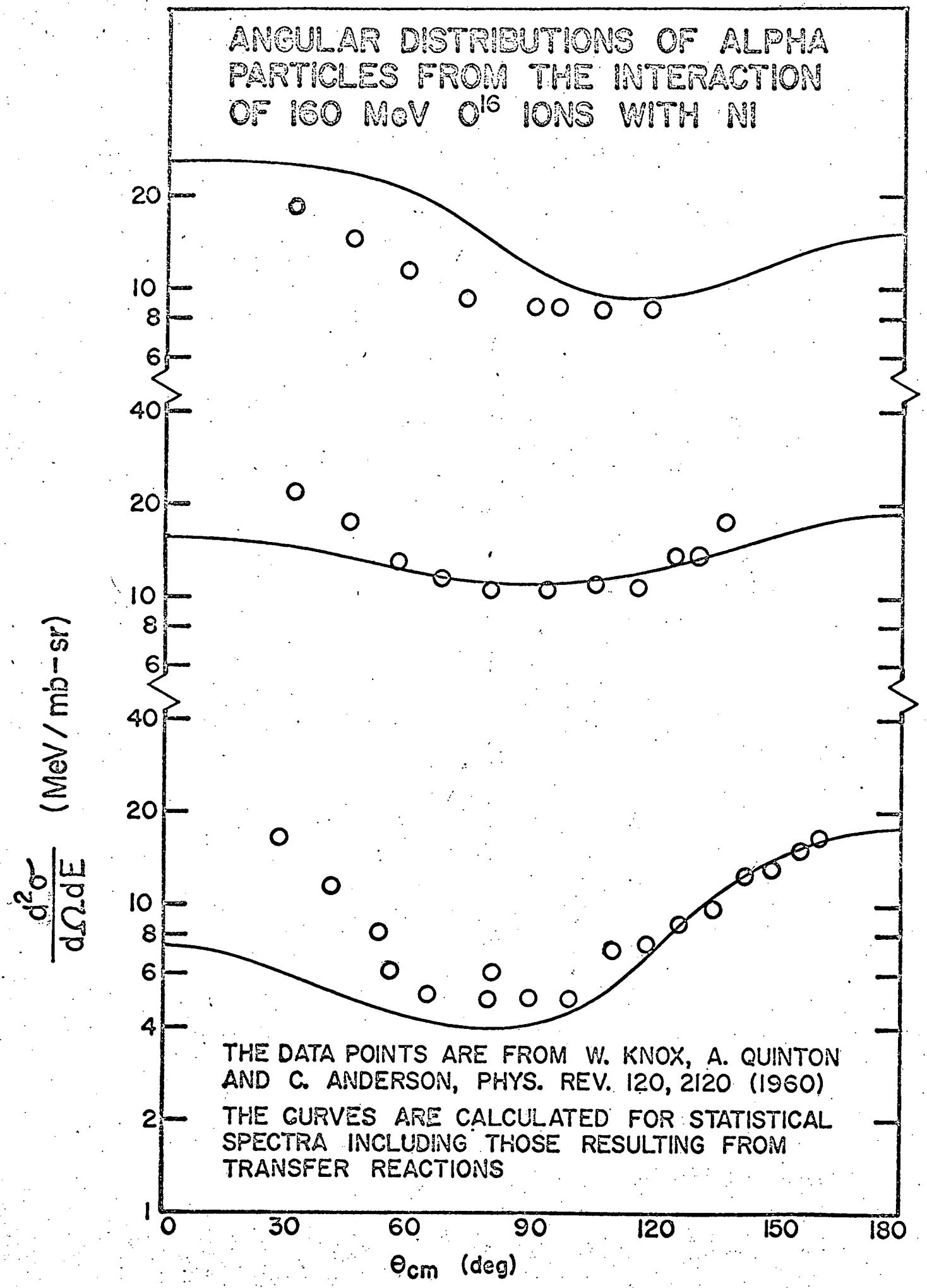
ANGULAR DISTRIBUTIONS OF ALPHA PARTICLES FROM THE INTERACTION OF 160 MeV O16 IONS WITH Ni
20
10
8
6
40
20
10
8
6
40
20
10
8
6
4
2
1
0
30
60
90
120
150
180
θcm (deg)
d²σ/dΩ.dE (MeV/mb-sr)
THE DATA POINTS ARE FROM W. KNOX, A. QUINTON AND C. ANDERSON, PHYS. REV. 120, 2120 (1960)
THE CURVES ARE CALCULATED FOR STATISTICAL SPECTRA INCLUDING THOSE RESULTING FROM TRANSFER REACTIONS

AMOUNT OF VARIOUS ISOTOPES PRODUCED FROM THE DECAY OF 10000 GE 67 COMPOUND NUCLEI
FORMED BY THE BOMBARDMENT OF ZN 64 WITH 37.7 MEV HE 3

GE 63	GE 64	GE 65	GE 66	GE 67
IN= 0.	IN= 16.	IN= 503.	IN= 3100.	IN=10000.
OUT= 0.	OUT= 8.	OUT= 501.	OUT= 3100.	OUT=10000.
LEFT= 0.	LEFT= 8.	LEFT= 2.	LEFT= 0.	LEFT= 0.

GA 62	GA 63	GA 64	GA 65	GA 66
IN= 0.	IN= 12.	IN= 2053.	IN= 5929.	IN= 6900.
OUT= 0.	OUT= 0.	OUT= 1169.	OUT= 5905.	OUT= 6900.
LEFT= 0.	LEFT= 12.	LEFT= 884.	LEFT= 24.	LEFT= 0.

ZN 61	ZN 62	ZN 63	ZN 64	ZN 65
IN= 0.	IN= 0.	IN= 1793.	IN= 6998.	IN= 3568.
OUT= 0.	OUT= 0.	OUT= 0.	OUT= 2808.	OUT= 3517.
LEFT= 0.	LEFT= 0.	LEFT= 1793.	LEFT= 4190.	LEFT= 51.

CU 60	CU 61	CU 62	CU 63	CU 64
IN= 0.	IN= 0.	IN= 0.	IN= 2321.	IN= 856.
OUT= 0.	OUT= 0.	OUT= 0.	OUT= 0.	OUT= 146.
LEFT= 0.	LEFT= 0.	LEFT= 0.	LEFT= 2321.	LEFT= 710.

NI 59	NI 60	NI 61	NI 62	NI 63
IN= 0.	IN= 0.	IN= 0.	IN= 0.	IN= 5.
OUT= 0.	OUT= 0.	OUT= 0.	OUT= 0.	OUT= 0.
LEFT= 0.	LEFT= 0.	LEFT= 0.	LEFT= 0.	LEFT= 5.

Fig VIII-1

Amount of Various Isotopes Produced From the Decay of 10000 Ge67 Compound Nuclei Formed by the Bombardment of Zn^{64} with He^3 of Several Different Energies

Energy of He^3(MeV)

	15	17.5	20	25	30	35	37.7	40	42
Ge67	0	0	0	0	0	0	0	0	0
Ge66	41	19	5	1	0	0	0	0	0
Ga66	387	166	62	5	0	0	0	0	0
Ge65	31	105	178	79	16	3	2	1	0
Ga65	5374	5652	4862	1425	276	29	24	12	7
Zn65	4167	3977	3730	1965	678	122	51	17	13
Ge64	0	0	0	0	1	9	8	7	5
Ga64	0	0	0	353	1279	1367	844	641	428
Zn64	0	81	1012	5383	7071	5765	4190	3044	2059
Cu64	0	0	152	790	603	752	710	602	469
Ge63	0	0	0	0	0	0	0	0	0
Ga63	0	0	0	0	0	1	12	36	76
Zn63	0	0	0	0	27	610	1793	2719	3625
Cu63	0	0	0	0	50	1336	2321	2912	3300
Ni63	0	0	0	0	0	7	5	10	18

Note: The total of each column is 10,000.

Figure VIII - 2

Amount of Various Isotopes Produced from the Decay of 10000 Ge69 Compound Nuclei formed by the Bombardment of Zn^{66} with He^3 of Several Different Energies

Energy of He^3 (MeV)

	15	17.5	20	25	30	35	37.7	40	42
Ge67	0	0	0	0	0	0	0	0	0
Ge68	262	55	18	1	0	0	0	0	0
Ga68	218	82	19	2	0	0	0	0	0
Ge67	1729	2064	1291	547	129	36	8	6	2
Ga67	7315	7182	4970	2072	409	38	19	5	2
Zn67	476	520	573	464	137	26	14	4	2
Ge66	0	0	0	49	274	209	136	111	69
Ga66	0	0	922	3612	5842	4081	3409	2575	1769
Zn66	0	97	2206	3247	2962	2437	2232	1431	999
Cu66	0	0	0	4	16	35	41	41	35
Ge65	0	0	0	0	0	0	1	4	10
Ga65	0	0	0	0	6	411	874	1444	2005
Zn65	0	0	0	0	222	2499	3169	3949	4683
Cu65	0	0	0	0	2	288	71	429	424
Ni65	0	0	0	0	0	0	0	0	0

Note: The total of each column is 10,000.

Figure VIII - 3

Fig IX-1

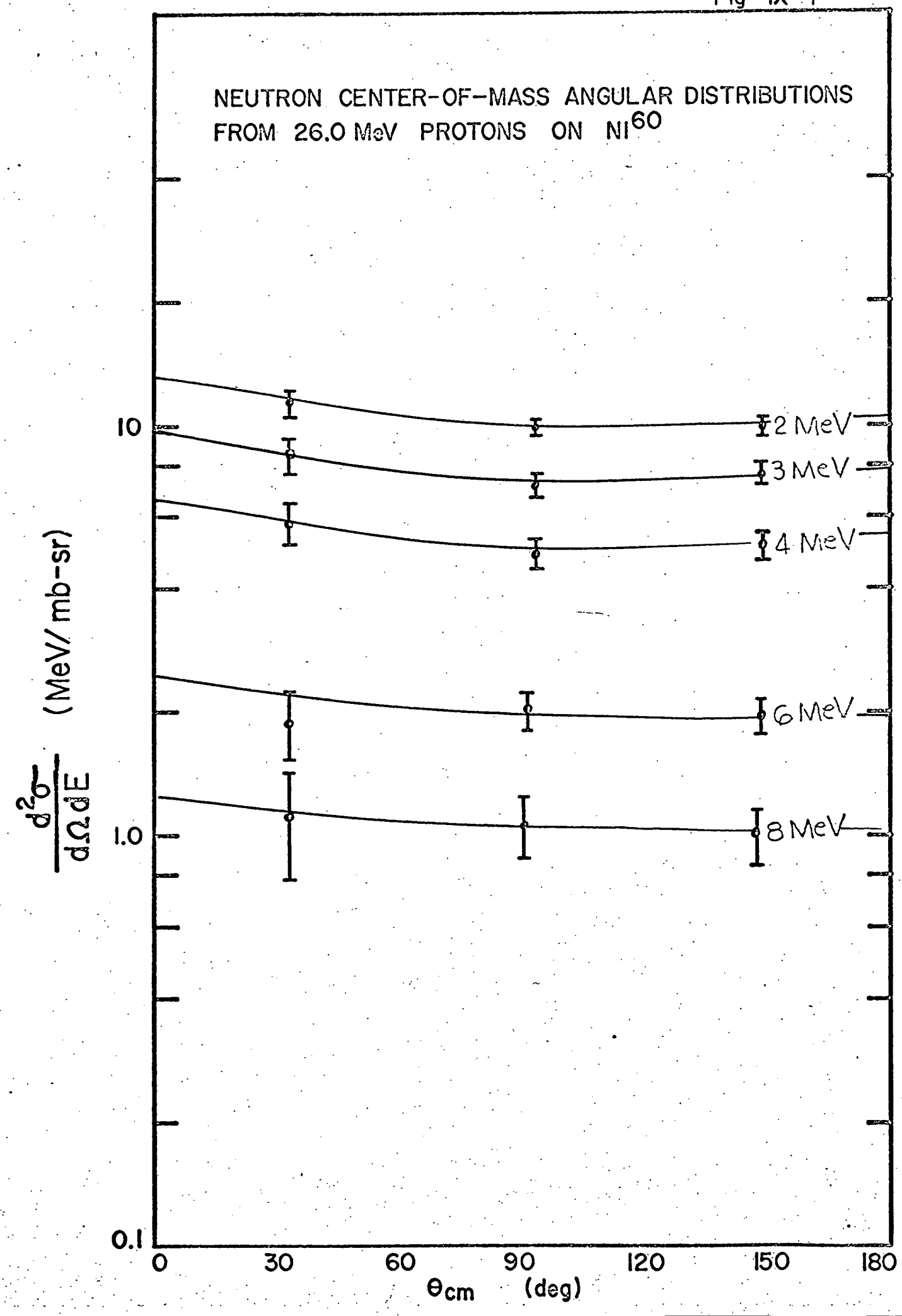
NEUTRON CENTER-OF-MASS ANGULAR DISTRIBUTIONS
FROM 26.0 MeV PROTONS ON Ni60
10
1.0
0.1
d2σ/dΩdE (MeV/mb-sr)
2 MeV
3 MeV
4 MeV
6 MeV
8 MeV
0
30
60
90
120
150
180
θcm (deg)

Fig IX-2

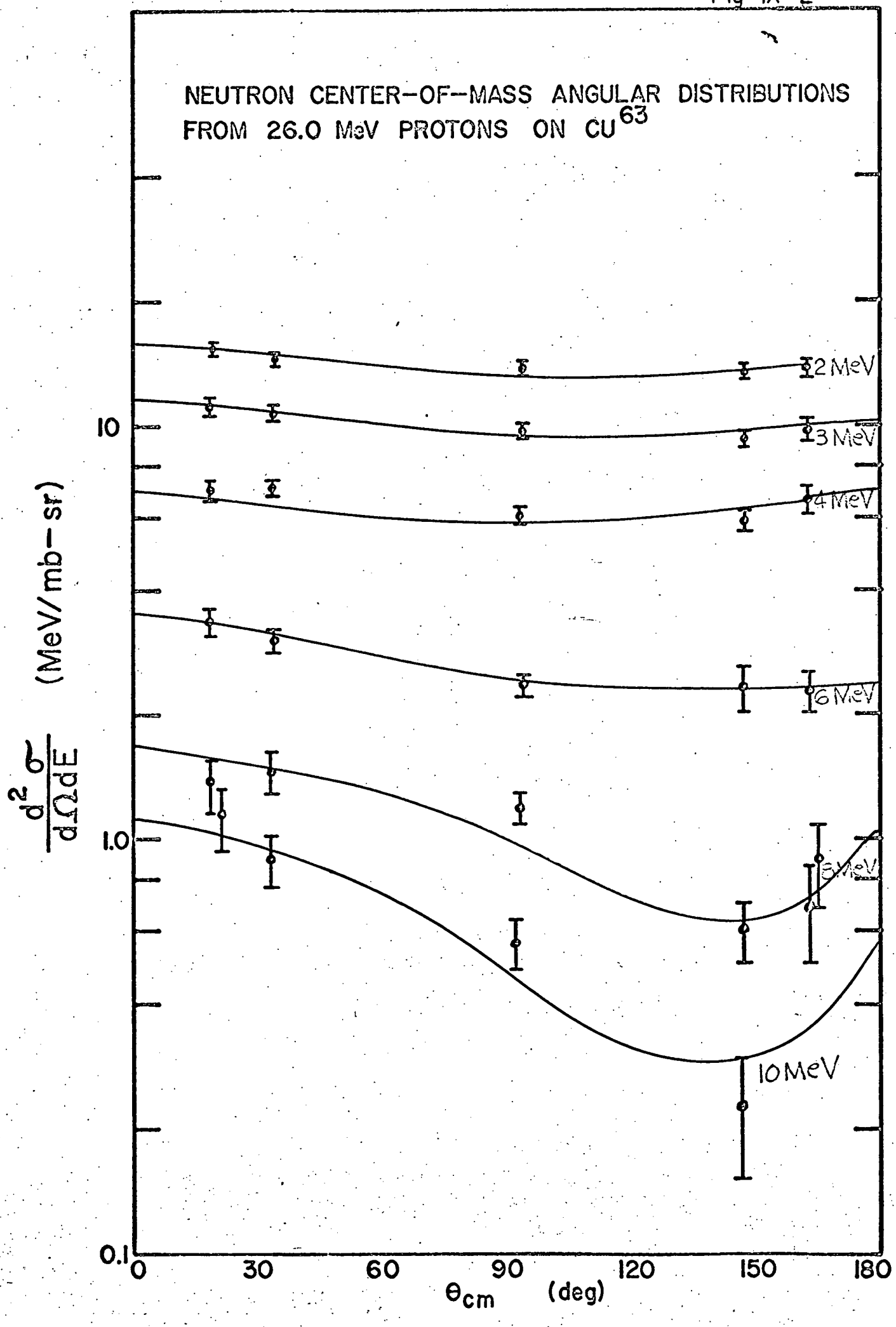
NEUTRON CENTER-OF-MASS ANGULAR DISTRIBUTIONS
FROM 26.0 MeV PROTONS ON CU63
d²σ/dΩdE (MeV/mb-sr)
10
1.0
0.1
2 MeV
3 MeV
4 MeV
6 MeV
8 MeV
10 MeV
0
30
60
90
120
150
180
θcm (deg)

Fig IX-3

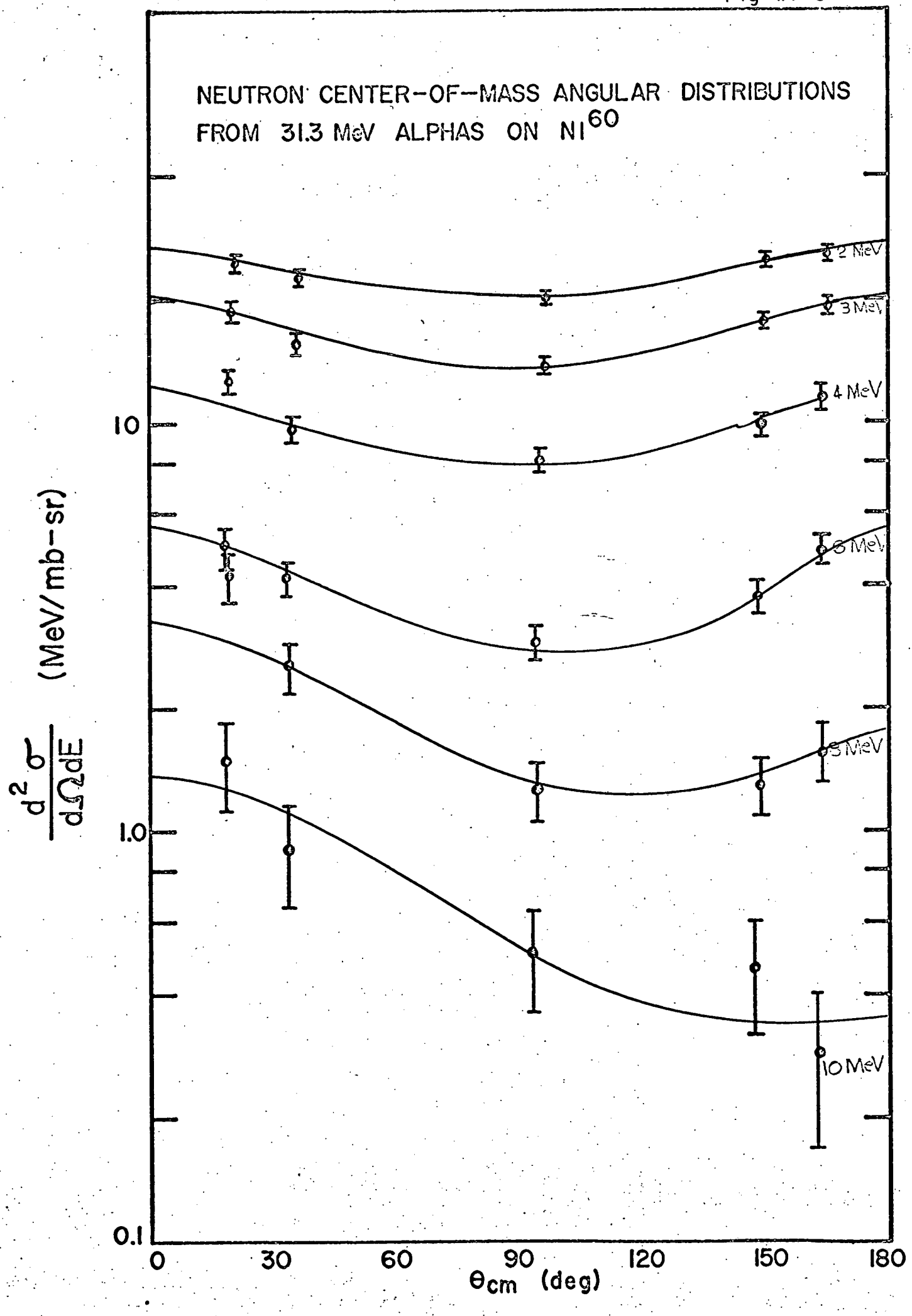
NEUTRON CENTER-OF-MASS ANGULAR DISTRIBUTIONS
FROM 31.3 MeV ALPHAS ON Ni60
2 MeV
3 MeV
4 MeV
6 MeV
8 MeV
10 MeV
10
1.0
0.1
d²σ/dΩdE (MeV/mb-sr)
0
30
60
90
120
150
180
θcm (deg)

Fig IX-4

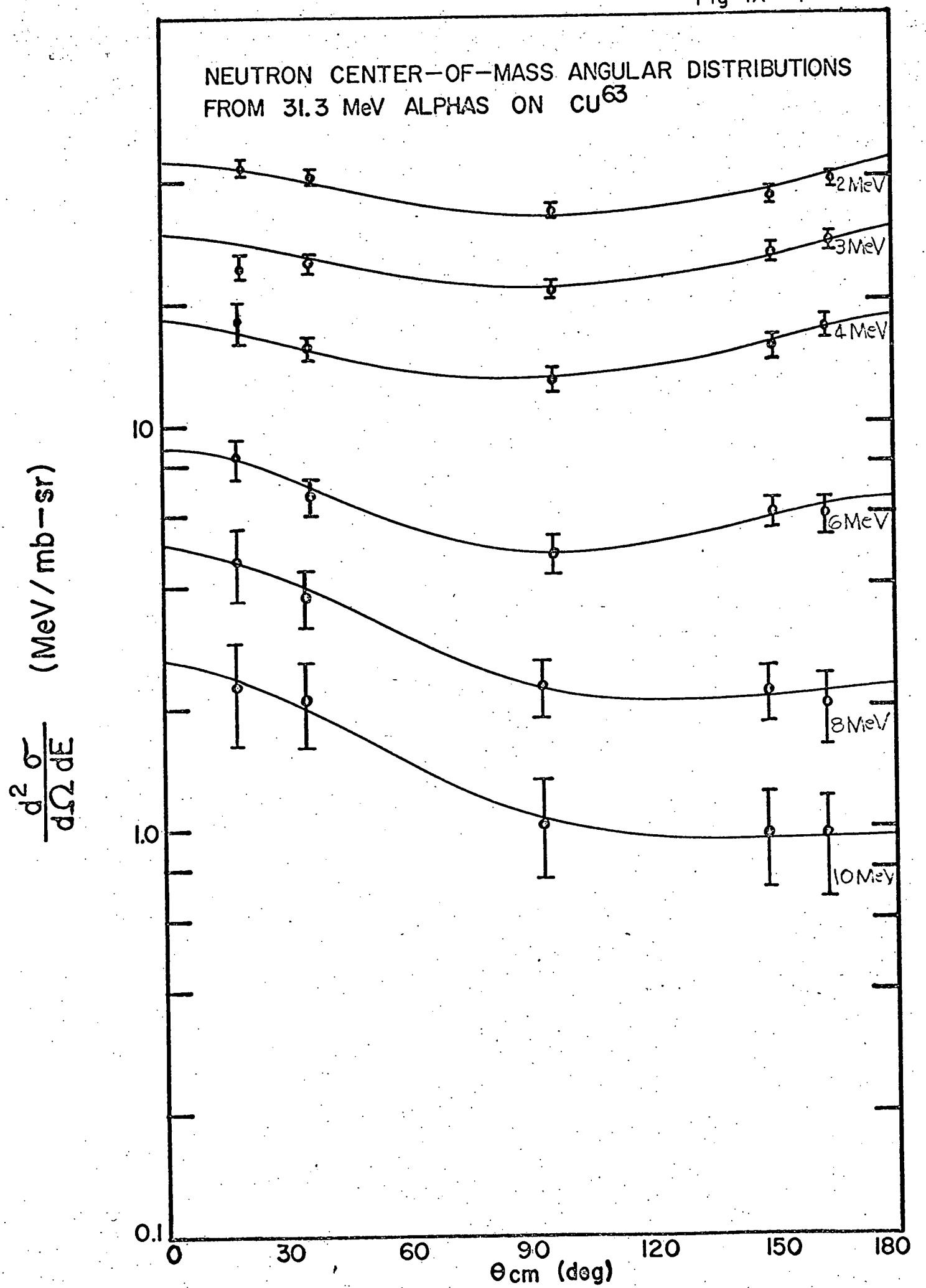
NEUTRON CENTER-OF-MASS ANGULAR DISTRIBUTIONS
FROM 31.3 MeV ALPHAS ON Cu^{63}
2 MeV
3 MeV
4 MeV
6 MeV
8 MeV
10 MeV
10
1.0
0.1
$\frac{d^2\sigma}{d\Omega\, dE}$ (MeV/mb-sr)
0
30
60
90
120
150
180
θcm (deg)

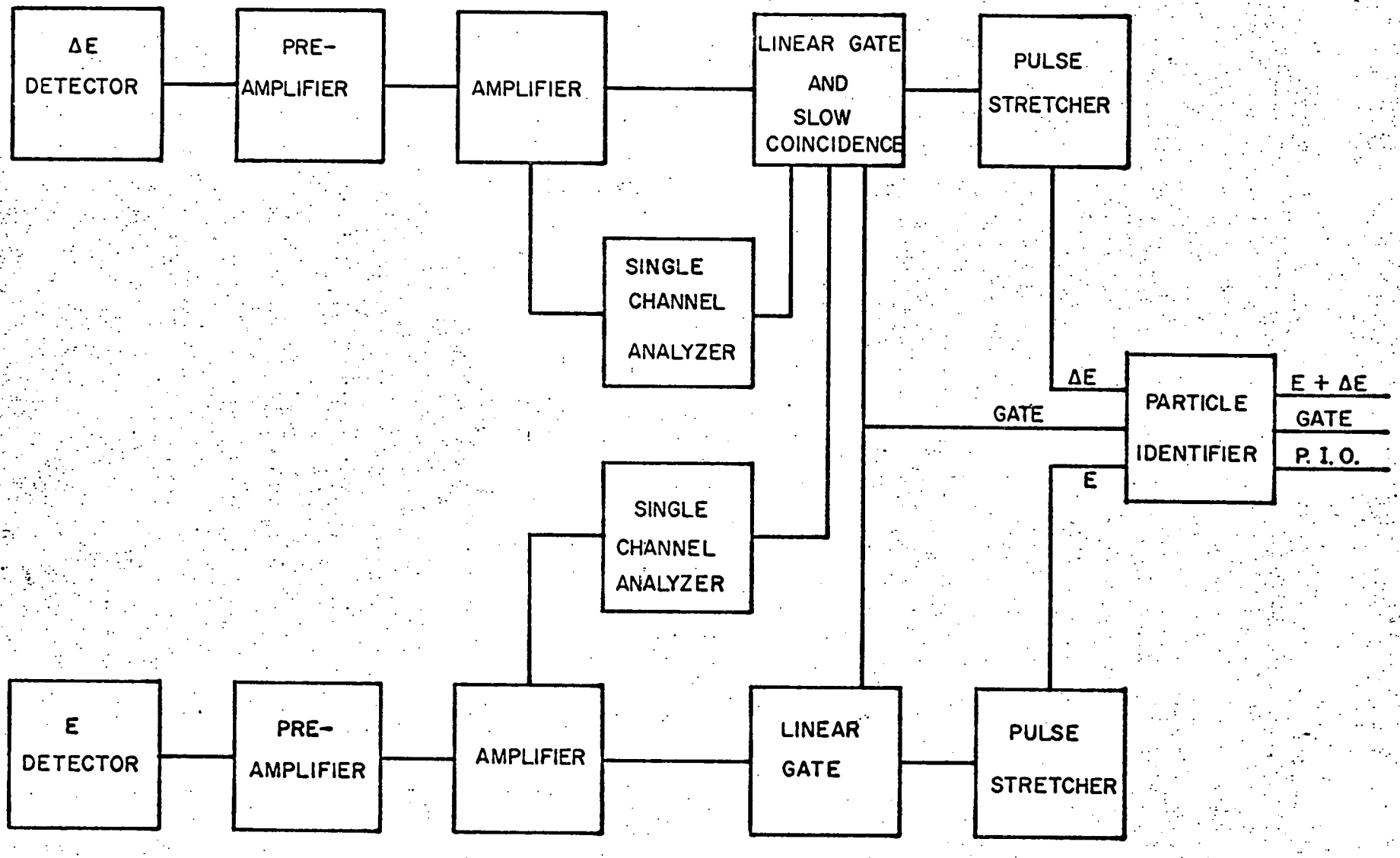

CHARGED PARTICLE SPECTROMETER

Fig X-1

DE DETECTOR THICKNESS = 20 MICRONS

Incident Energy	P.I.O. Proton	P.I.O. Deuteron	P.I.O. Triton	P.I.O. Helium Three	P.I.O. Helium Four
0.5	3.83	3.83	3.83	3.95	3.95
1.0	2.39	2.39	2.39	2.39	2.30
1.5	2.30	4.51	4.87	4.87	4.87
2.0	2.00	3.61	5.06	8.08	8.08
2.5	1.88	3.30	4.55	11.97	11.97
3.0	1.82	3.16	4.31	16.50	16.50
3.5	1.79	3.07	4.18	21.65	21.65
4.0	1.76	3.02	4.10	27.38	27.38
4.5	1.75	2.98	4.05	23.92	31.62
5.0	1.74	2.96	4.01	21.84	28.54
5.5	1.73	2.94	3.98	20.57	26.54
6.0	1.72	2.92	3.96	19.70	25.22
6.5	1.72	2.91	3.95	19.07	24.29
7.0	1.72	2.90	3.94	18.60	23.59
7.5	1.71	2.90	3.93	18.23	23.05
8.0	1.71	2.89	3.92	17.93	22.62
8.5	1.71	2.89	3.91	17.69	22.28
9.0	1.71	2.88	3.91	17.50	22.00
9.5	1.71	2.88	3.90	17.33	21.76
10.0	1.71	2.88	3.90	17.19	21.57
11.0	1.72	2.88	3.89	16.96	21.25
12.0	1.72	2.87	3.89	16.79	21.01
13.0	1.72	2.87	3.89	16.66	20.83
14.0	1.73	2.87	3.89	16.55	20.68
15.0	1.73	2.87	3.89	16.47	20.57
16.0	1.74	2.88	3.89	16.80	20.47
17.0	1.74	2.88	3.89	16.33	20.39
18.0	1.75	2.88	3.89	16.28	20.32
19.0	1.75	2.88	3.89	16.24	20.27
20.0	1.76	2.88	3.89	16.20	20.22

Figure X - 2

DE DECTOR THICKNESS = 40 MICRONS

Incident Energy	P.I.O. Proton	P.I.O. Deuteron	P.I.O. Triton	P.I.O. Helium Three	P.I.O. Helium Four
0.5	0.70	0.70	0.70	0.70	0.70
1.0	2.39	2.39	2.39	2.39	2.39
1.5	4.87	4.87	4.87	4.87	4.87
2.0	5.57	8.08	8.08	8.08	8.08
2.5	4.50	9.52	11.97	11.97	11.97
3.0	4.11	7.84	11.78	16.50	16.50
3.5	3.90	7.16	10.33	21.65	21.65
4.0	3.77	6.79	9.61	27.38	27.38
4.5	3.69	6.55	9.17	33.69	33.69
5.0	3.63	6.38	8.88	40.55	40.55
5.5	3.59	6.26	8.68	47.96	47.96
6.0	3.56	6.17	8.52	55.90	55.90
6.5	3.54	6.11	8.41	59.12	64.35
7.0	3.52	6.05	8.32	51.78	73.32
7.5	3.50	6.01	8.24	47.69	66.61
8.0	3.49	5.97	8.18	44.98	61.08
8.5	3.49	5.94	8.14	43.01	57.44
9.0	3.48	5.92	8.09	41.52	54.82
9.5	3.48	5.90	8.06	40.34	52.83
10.0	3.47	5.88	8.03	39.39	51.26
11.0	3.47	5.86	7.98	37.94	48.93
12.0	3.47	5.84	7.95	36.90	47.29
13.0	3.47	5.82	7.92	36.11	46.08
14.0	3.48	5.81	7.90	35.50	45.14
15.0	3.49	5.81	7.88	35.02	44.41
16.0	3.49	5.80	7.87	34.63	43.82
17.0	3.50	5.80	7.86	34.30	43.33
18.0	3.51	5.80	7.85	34.03	42.92
19.0	3.52	5.80	7.85	33.80	42.58
20.0	3.53	5.80	7.84	33.60	42.29

Figure X - 3

DE DETECTOR THICKNESS = 60 MICRONS

Incident Energy	P.I.O. Proton	P.I.O. Deuteron	P.I.O. Triton	P.I.O. Helium Three	P.I.O. Helium Four
0.5	0.70	0.70	0.70	0.70	0.70
1.0	2.39	2.39	2.39	2.39	2.39
1.5	4.87	4.87	4.87	4.87	4.87
2.0	8.08	8.08	8.08	8.08	8.08
2.5	8.90	11.97	11.97	11.97	11.97
3.0	7.14	16.50	16.50	16.50	16.50
3.5	6.47	13.22	21.65	21.65	21.65
4.0	6.10	11.72	17.88	27.38	27.38
4.5	5.87	10.92	16.04	33.69	33.69
5.0	5.71	10.41	15.00	40.55	40.55
5.5	5.60	10.06	14.32	47.96	47.96
6.0	5.52	9.81	13.85	55.90	55.90
6.5	5.46	9.62	13.50	64.35	64.35
7.0	5.41	9.47	13.23	73.32	73.32
7.5	5.37	9.36	13.02	82.79	82.79
8.0	5.34	9.26	12.85	92.74	92.74
8.5	5.32	9.18	12.71	89.47	103.19
9.0	5.30	9.12	12.59	79.96	114.11
9.5	5.29	9.07	12.50	74.28	108.62
10.0	5.28	9.02	12.41	70.33	98.84
11.0	5.26	8.95	12.28	65.08	88.03
12.0	5.26	8.90	12.18	61.68	81.82
13.0	5.25	8.86	12.10	59.29	77.70
14.0	5.26	8.83	12.04	57.51	74.74
15.0	5.26	8.80	12.00	56.14	72.52
16.0	5.27	8.79	11.96	55.06	70.78
17.0	5.28	8.78	11.93	54.18	69.39
18.0	5.29	8.77	11.90	53.45	68.26
19.0	5.30	8.76	11.88	52.85	67.31
20.0	5.32	8.76	11.87	52.34	66.52

Figure X - 4

DE DETECTOR THICKNESS = 80 MICRONS

Incident Energy	P.I.O. Proton	P.I.O. Deuteron	P.I.O. Triton	P.I.O. Helium Three	P.I.O. Helium Four
0.5	0.70	0.70	0.70	0.70	0.70
1.0	2.39	2.39	2.39	2.39	2.39
1.5	4.87	4.87	4.87	4.87	4.87
2.0	8.08	8.08	8.08	8.08	8.08
2.5	11.97	11.97	11.97	11.97	11.97
3.0	11.81	16.50	16.50	16.50	16.50
3.5	9.72	21.65	21.65	21.65	21.65
4.0	8.84	19.03	27.38	27.38	27.38
4.5	8.33	16.56	595.74	33.69	33.69
5.0	8.01	15.29	23.23	40.55	40.55
5.5	7.78	14.48	21.38	47.96	47.96
6.0	7.62	13.93	20.21	55.90	55.90
6.5	7.49	13.52	19.40	64.35	64.35
7.0	7.40	13.22	18.80	73.32	73.32
7.5	7.32	12.98	18.34	82.79	82.79
8.0	7.27	12.79	17.97	92.74	92.74
8.5	7.22	12.63	17.68	103.19	103.19
9.0	7.18	12.50	17.44	114.11	114.11
9.5	7.15	12.39	17.24	125.50	125.50
10.0	7.13	12.30	17.07	127.43	137.36
11.0	7.09	12.16	16.80	104.06	162.44
12.0	7.07	12.05	16.60	93.95	133.35
13.0	7.06	11.97	16.45	87.83	120.12
14.0	7.06	11.91	16.33	83.63	112.11
15.0	7.06	11.86	16.23	80.56	106.60
16.0	7.07	11.83	16.15	78.21	102.55
17.0	7.08	11.80	16.09	76.36	99.43
18.0	7.09	11.78	16.04	74.86	96.96
19.0	7.10	11.77	15.99	73.63	94.95
20.0	7.12	11.76	15.96	72.60	93.29

Figure X - 5